

Searching for minicharged particles via birefringence, dichroism and Raman spectroscopy of the vacuum polarized by a high-intensity laser wave

S. Villalba-Chávez, C. Müller

*Institut für Theoretische Physik I, Heinrich Heine Universität Düsseldorf
Universitätsstr. 1, 40225 Düsseldorf, Germany*

Abstract

Absorption and dispersion of probe photons in the field of a high-intensity circularly polarized laser wave are investigated. The optical theorem is applied for determining the absorption coefficients in terms of the imaginary part of the vacuum polarization tensor. Compact expressions for the vacuum refraction indices and the photon absorption coefficients are obtained in various asymptotic regimes of interest. The outcomes of this analysis reveal that, far from the region relatively close to the threshold of the two-photon reaction, the birefringence and dichroism of the vacuum are small and, in some cases, strongly suppressed. On the contrary, in a vicinity of the region in which the photo-production of a pair occurs, these optical properties are manifest with lasers of moderate intensities. We take advantage of such a property in the search of minicharged particles by considering high-precision polarimetric experiments. In addition, Raman-like electromagnetic waves resulting from the inelastic part of the vacuum polarization tensor are suggested as an alternative form for finding exclusion limits on these hypothetical charge carriers. The envisaged parameters of upcoming high-intensity laser facilities are used for establishing upper bounds on the minicharged particles.

Keywords: Beyond Standard Model, Vacuum Polarization, Laser Fields, Minicharged Particles.

PACS: 12.20.-Fv, 14.80.-j

1. Introduction

Investigating the frontiers of the Standard Model (SM) is a fundamental issue in elementary particle physics. Despite the successes of the minimal $SU(3) \times SU(2) \times U(1)$ gauge group as unified description of the strong and electro-weak interaction, there still remain a variety of nontrivial issues whose solutions often demand physics beyond the SM. The absence of a satisfactory explanation for the large number of free parameters as well as the hierarchy and naturalness problems to which they are subject constitute clear examples of unresolved questions. These seem to be direct consequences of dealing with an effective formulation rather than a fundamental theory where, among other issues, gravity is conceptually reconciled with the remaining interactions. In connection, several SM extensions have been put forward. At energies much above the typical SM scale—specified by the mass of the W_{\pm} -bosons—supersymmetric versions and string theory are likely to occur [1, 2]. In contrast, below the scale given by the electron mass m , the promising candidates introduce weakly interacting sectors [3, 4, 5, 6], sometimes, with additional $U(1)$ invariance often resulting from string compactifications [7, 8]. As a consequence, hypothetical paraphotons [9, 10, 11, 12, 13]—kinematically mixed with the visible $U(1)$ sector—are promoted and light particles with tiny fractions of the electron charge are suspected to occur in nature [14, 15, 16, 17, 18]. Models which rely on these kind of minicharged particles (MCPs) are of paramount importance in contemporary physics since they constitute by themselves ideal frameworks for probing the validity of the SM, the theoretical conception of magnetic monopoles and, therefore, the highly nontrivial principle of charge quantization.

Email addresses: selym@tp1.uni-duesseldorf.de (S. Villalba-Chávez), c.mueller@tp1.uni-duesseldorf.de (C. Müller)

Over the last decade there have been considerable experimental efforts toward the exploration of the low energy frontiers of particle physics, mainly through the unconventional properties of the unstable and nonlinear vacuum of Quantum Electrodynamics (QED). Indeed, polarimetric experiments with unprecedented levels of sensitivity represent a powerful tool for finding out stringent constraints on the parameters associated with weakly interacting particles [19, 20, 21, 22]. The reasons for using these optical setups follows from a hypothetical coupling between the MCPs and a constant magnetic field. In such a context, the interaction would induce modifications on the dichroic and birefringent properties of the vacuum [23, 24, 25, 26, 27, 28], a fact which constitutes a potential signal of their existences. Also high-precision photon regenerative experiments have been carried out in several collaborations [29, 30, 31, 32, 33, 34, 35, 36]. Most of them relied on a “Light Shining Through a Wall” setup [37, 38, 39, 40, 41], where the photon oscillation into a weakly interacting particle allows for traversing a photon blocker barrier and, eventually, its regeneration behind the wall. In both types of experiments a tiny effect due to the MCPs is expected, but they might be more manifest by increasing the magnetic field strength and its spatial extension. Nowadays, it is not a big issue to extend the effective interaction region up to a few kilometers by using mirrors of extremely high reflectivity. In contrast, the attainable magnetic field strengths still remain nine orders of magnitude smaller than the critical one of QED [$B_c = 4.42 \times 10^{13}$ G], near of which, the upper bounds on MCPs are expected to be quite stringent.

With the progressive increasing of the available intensity, laser technology is becoming a competitive source of strong fields, valuable for the search of MCPs. Projects such as the Extreme Light Infrastructure (ELI) [42] and the Exawatt Center for Extreme Light Studies (XCELS) [43] are being designed to reach fields of about two orders of magnitude below the critical one in ultra-short pulses of temporal lengths of the order of $\tau \approx 10$ fs. Hence, the prospect of finding stringent limits on the MCPs by using high-intensity lasers is certainly enticing. Obviously, an essential step in this direction is achieved by knowing the expressions of the vacuum polarization tensor in the field of a plane-wave. Although these were derived a long time ago [44, 45], up to now their main essential consequence considered in a realistic context remains the production of electron-positron pairs by a photon—also known as the Breit-Wheeler reaction—[46, 47, 48, 49, 50, 51], and in the Coulomb field of a nucleus, i.e., the Bethe-Heitler phenomenon [52, 53]. So far, the production rates of the latter processes have not found a direct application in the search of MCPs. In contrast, the optical properties of a polarized QED vacuum are those which might provide sensitive insights on the parameters associated with these hypothetical charge carriers. Previous considerations on the optical nature of the vacuum, polarized by a circularly polarized laser, were partially developed in Ref. [45], where a numerical assessment of the photon absorption coefficients and the vacuum refraction indices was undertaken in regions different from the strong field regime.

In contrast to this numerical study, we determine in the present work analytical expressions for the vacuum refraction indices and the photon absorption coefficients in various asymptotic domains, including the one related to the strong field domain. Besides, the study of these optical quantities is extended to the framework of scalar QED since the spinless realization of MCPs is not discarded [54, 55]. We show that, far from the threshold of two-photon reaction—and independently of the nature of the charge carriers—the birefringence and dichroism properties of the vacuum are small, and in some regions, strongly suppressed. On the contrary, in a vicinity of the first photo-production threshold, the birefringence and dichroism of the vacuum are considerably more pronounced. Both phenomena are closely connected with the chiral activity of the “medium” and—according to our results—could be observed even at intensities available today. We take advantage of such a property in the search of MCPs by considering high-precision polarimetric techniques. Because of the relative weakness of the aforementioned phenomenon in the strong field regime, we look for an observable different from the ellipticity and the rotation of the polarization plane, both frequently considered in the case where a dipole magnet drives the polarization of the vacuum. In fact, we take into account Raman-like electromagnetic waves arising from the inelastic interaction in the photon-photon scattering. The associated spectroscopy techniques are then suggested for probing the quantum vacuum but also for determining upper bounds on the parameters intrinsically associated with the MCPs.

2. Photon scattering in a circularly polarized wave

2.1. The polarization tensor, its tensorial structure and form factors

We are motivated to investigate the effects induced by hypothetical particles characterized by a mass m_ϵ and a tiny fraction of the electron charge $q_\epsilon \equiv e|e|$. As long as the energy scale remains within the phenomenological limits

of QED and its fundamental principles are preserved, the consequences associated with the existence of this sort of MCPs would not differ from those emerging in a pure QED context. Conceptually, one can then investigate the related phenomenology from the already known expressions, with the electron parameters (e , m) substituted by the respective quantities associated with an MCP (q_ϵ , m_ϵ). Besides, by probing the nonlinear and unstable properties of the $q_\epsilon^+ q_\epsilon^-$ vacuum in an external background field, stringent limits on the presumable smallness of the unknown parameters ϵ and m_ϵ can be obtained. This constitutes a motivation for studying the dispersive and absorptive processes intrinsically connected to the vacuum polarization effects. The latter become primarily manifest in the generating functional of one-particle irreducible diagrams

$$\Gamma = \frac{1}{8\pi} \int d^4x d^4x' \left\{ a_\mu(x) \left[\left(\square g^{\mu\nu} - \partial^\mu \partial^\nu \right) \delta^4(x-x') + \Pi^{\mu\nu}(x, x') \right] a_\nu(x') \right\} + \dots \quad (1)$$

where the metric tensor reads $g_{\mu\nu} = \text{diag}(+1, -1, -1, -1)$, $\square \equiv \partial_\mu \partial^\mu = \partial^2 / \partial t^2 - \nabla^2$ and the abbreviation $+\dots$ stands for higher order terms in the small-amplitude electromagnetic wave $a_\mu(x)$. The respective Dyson-Schwinger equation [56, 57, 58, 59, 60], written up to linear order in $a_\mu(x)$, has the form

$$\square a_\mu(x) + \int d^4x' \Pi_{\mu\nu}(x, x') a^\nu(x') = 0 \quad (2)$$

provided that $a_\mu(x)$ is chosen in the Lorenz gauge $\partial a = 0$. While the first term in Eq. (2) is the classical Maxwell contribution, the second one is responsible for the interaction of photons with the external background field. Such an interaction is mediated by the virtual minicharged carriers and encompassed in the vacuum polarization tensor $\Pi_{\mu\nu}(x, x')$. It is through this object that the gauge sector of QED acquires a dependence on the strong field of the wave. The latter is taken hereafter as a circularly polarized monochromatic plane-wave¹

$$\mathcal{A}^\mu(x) = a_1^\mu \cos(\varkappa x) + a_2^\mu \sin(\varkappa x) \quad \text{with} \quad a_1 a_2 = 0, \quad \varkappa^2 = 0, \quad a_1^2 = a_2^2 \equiv a^2, \quad (3)$$

and specialized in the Lorenz gauge $\partial \mathcal{A} = 0$ as well. This condition implies that the wave four-vector $\varkappa^\mu = (\varkappa^0, \varkappa)$ and the constant polarization vectors a_i^μ (with $i = 1, 2$) satisfy the constraints $\varkappa a_i = 0$. With these details in mind, we Fourier transform Eq. (2)

$$k_1^2 a_\mu(k_1) - \int \frac{d^4k_2}{(2\pi)^4} \Pi_{\mu\nu}(k_1, k_2) a^\nu(k_2) = 0, \quad (4)$$

and consider the one-loop approximation in $\Pi_{\mu\nu}(k_1, k_2)$, in which case the polarization tensor acquires the following structure (for details we refer the reader to Ref. [44])

$$\Pi^{\mu\nu}(k_1, k_2) = (2\pi)^4 \delta^4(k_1 - k_2) \Pi_0^{\mu\nu}(k_2) + (2\pi)^4 \delta^4(k_1 - k_2 + 2\varkappa) \Pi_+^{\mu\nu}(k_2) + (2\pi)^4 \delta^4(k_1 - k_2 - 2\varkappa) \Pi_-^{\mu\nu}(k_2). \quad (5)$$

The tensorial objects involved in this expression can be expanded in terms of the following Lorentz covariant vectors

$$\Lambda_\pm^\mu(k) = -\frac{(\mathcal{F}_1^{\mu\nu} \pm i \mathcal{F}_2^{\mu\nu}) k_\nu}{(k\varkappa)(-a^2)^{1/2}}, \quad \Lambda_3^\mu(k) = \frac{\varkappa^\mu k^2 - k^\mu (k\varkappa)}{(k\varkappa)(k^2)^{1/2}} \quad (6)$$

where $\mathcal{F}_i^{\mu\nu} = \varkappa^\mu a_i^\nu - \varkappa^\nu a_i^\mu$ denotes the field strengths tensor associated with each external field mode ($i = 1, 2$). We emphasize that Eq. (6) does not depend on which choice of k is taken since the difference between k_1 and k_2 is proportional to \varkappa . Note that Λ_\pm are eigenstates of the helicity operator subject to the normalization conditions $\Lambda_+ \Lambda_- = -2$ with $\Lambda_\pm \Lambda_\pm = 0$. Besides, we also find that $\Lambda_3 \Lambda_3 = -1$ with $\Lambda_\pm \Lambda_3 = 0$. With Eq. (6) in mind, the part in Eq. (5) responsible for the elastic scattering can be written as

$$\Pi_0^{\mu\nu}(k_1) = \frac{1}{2}(\pi_3 + i\pi_1) \Lambda_+^\mu \Lambda_-^\nu + \frac{1}{2}(\pi_3 - i\pi_1) \Lambda_-^\mu \Lambda_+^\nu + \pi_5 \Lambda_3^\mu \Lambda_3^\nu, \quad (7)$$

¹From now on “natural” and Gaussian units $c = \hbar = 4\pi\epsilon_0 = 1$ are used.

whereas the tensors associated with inelastic scattering turn out to be $\Pi_{\pm}^{\mu\nu}(k_1) = \pi_0 \Lambda_{\pm}^{\mu} \Lambda_{\pm}^{\nu}$. These inelastic scattered waves emerge as a consequence of the simultaneous emission or absorption of photons of the high-intensity laser wave upon the scattering event. As a matter of fact, they turn out to be shifted to lower or higher values in comparison with the original monochromatic frequency. The scattering of light in these latter two cases is analogous to Raman dispersion in molecular physics with \varkappa imitating the vibrational frequency of the molecules. Its relevance will be analyzed separately in Sec. 5.3.

It is worth emphasizing that, owing to Eq. (6), the polarization tensor satisfies not only the fundamental principles of charge conjugation, time reversal and parity symmetry but also the gauge invariance properties of the electromagnetic interaction. The form factors π_i involved in Eq. (7) turn out to be twofold parametric integrals²

$$\pi_i(\lambda_{\epsilon}, \xi_{\epsilon}) = -\frac{\alpha_{\epsilon}}{2\pi} m_{\epsilon}^2 \int_{-1}^1 dv \int_0^{\infty} \frac{d\rho}{\rho} e^{-\frac{2i\rho}{|\lambda_{\epsilon}|(1-v^2)}} \left[1 + 2A\xi_{\epsilon}^2 - \frac{k_1 k_2 (1-v^2)}{4m_{\epsilon}^2} \right] \Omega_i. \quad (8)$$

with

$$\begin{aligned} \Omega_1^{(0)} &= 2\xi_{\epsilon}^2 \rho A_0 \text{sign}[\lambda_{\epsilon}], & \Omega_1^{(\frac{1}{2})} &= 4\xi_{\epsilon}^2 \rho A_0 \frac{1+v^2}{1-v^2} \text{sign}[\lambda_{\epsilon}] \\ \Omega_5^{(0)} &= -\frac{k_1^2}{4m_{\epsilon}^2} v^2 (1 - e^{iy}), & \Omega_5^{(\frac{1}{2})} &= -\frac{k_1^2}{2m_{\epsilon}^2} (1-v^2) (1 - e^{iy}), \end{aligned} \quad (9)$$

$$\Omega_3^{(0)} = \xi_{\epsilon}^2 \sin^2(\rho) + \frac{1}{2} \left[1 - \frac{k_1^2}{4m_{\epsilon}^2} (1-v^2) \right] (1 - e^{iy}), \quad \Omega_3^{(\frac{1}{2})} = 2\xi_{\epsilon}^2 \sin^2(\rho) \frac{1+v^2}{1-v^2} - \left[1 + \frac{k_1^2}{4m_{\epsilon}^2} (1+v^2) \right] (1 - e^{iy}).$$

While the upper index 0 denotes the quantities coming out from a loop of scalar particles, the upper index $\frac{1}{2}$ refers to the case where the spin- $\frac{1}{2}$ representation mediates the interaction. Here $\alpha_{\epsilon} \equiv \epsilon^2 e^2 = \epsilon^2/137$ denotes the fine structure constant relative to the MCPs and $\xi_{\epsilon}^2 = -\epsilon^2 e^2 a^2/m_{\epsilon}^2$. Other functions and parameters, contained in these expressions, are given by

$$A = \frac{1}{2} \left(1 - \frac{\sin^2(\rho)}{\rho^2} \right), \quad A_0 = \frac{1}{2} \left(\frac{\sin^2(\rho)}{\rho^2} - \frac{\sin(2\rho)}{2\rho} \right), \quad A_1 = A + 2A_0, \quad y = \frac{4\rho\xi_{\epsilon}^2 A}{|\lambda_{\epsilon}|(1-v^2)}, \quad \lambda_{\epsilon} = \frac{\varkappa k}{2m_{\epsilon}^2}. \quad (10)$$

Because of the high-oscillatory behavior of the functions Ω_i , an exact analytical evaluation of the form factors π_i cannot be carried out. Instead, we shall focus ourselves on their asymptotic features in various limits of interest with respect to the parameters λ_{ϵ} and ξ_{ϵ} .

2.2. Dispersion and absorption of small-amplitude electromagnetic waves. General considerations.

The transversal small-amplitude electromagnetic wave, solution of Eq. (4), can be expressed as a superposition of two different helicity modes

$$a^{\mu}(k) = f_{+}(k)\Lambda_{+}^{\mu} + f_{-}(k)\Lambda_{-}^{\mu}. \quad (11)$$

In order to find their propagation laws we substitute Eq. (11) into Eq. (4) by inserting, in addition, Eq. (5) and Eq. (7). The resulting equation is projected onto the Λ_{\pm}^{μ} afterwards. The described procedure provides the following system of equations

$$\mathcal{G}^{(i)}(k)\mathbf{z}^{(i)}(k) = 0 \quad \text{with} \quad i = 1, 2. \quad (12)$$

Here the involved quantities are defined as follows:

$$\mathcal{G}^{(1)}(k) = \begin{bmatrix} k^2 + \pi_3 + i\pi_1 & 2\pi_0^+ \\ 2\pi_0 & (k + 2\varkappa)^2 + \pi_3^+ - i\pi_1^+ \end{bmatrix}, \quad \mathcal{G}^{(2)}(k) = \begin{bmatrix} (k - 2\varkappa)^2 + \pi_3^- + i\pi_1^- & 2\pi_0 \\ 2\pi_0^- & k^2 + \pi_3 - i\pi_1 \end{bmatrix}, \quad (13)$$

²The form factors defined in Eq. (8) and (9) are in correspondence with those obtained by Baier, Mil'shtein and Strakhovenko in Ref. [44] - according to the renaming rule $\pi_i \leftrightarrow \alpha_i$.

$$\mathbf{z}^{(1)} = \begin{bmatrix} f_+(k) \\ f_-(k+2\kappa) \end{bmatrix}, \quad \mathbf{z}^{(2)} = \begin{bmatrix} f_+(k-2\kappa) \\ f_-(k) \end{bmatrix}. \quad (14)$$

Note that the form factors having an upper index \pm must be evaluated at $k \rightarrow k \pm 2\kappa$. Because of this fact, both eigenproblems turn out to be correlated, i.e., $\mathcal{G}^{(2)}(k) = \mathcal{G}^{(1)}(k-2\kappa)$. Of course, the dispersion relations emerge whenever the determinant of $\mathcal{G}^{(i)}(k)$ vanishes identically. Its solutions can be determined by analytical procedures. However, we will consider the situation in which the polarization effects do not modify dramatically the usual photon dispersion law $\omega = |\mathbf{k}|$. Thereby only leading order corrections in α_ϵ will be taken into account. Guided by this approximation the relevant dispersion equations for $f_\pm(k)$ turn out to be

$$k^2 + \pi_3 \pm i\pi_1 \simeq 0, \quad (15)$$

where the contribution resulting from the off-diagonal terms in Eq. (13) has been neglected since it provides a correction smaller by a factor α_ϵ .

The polarization tensor $\Pi_{\mu\nu}$ is, in general, a non-hermitian object. In correspondence, its form factors contain real and imaginary contributions $\pi_i = \text{Re } \pi_i + i \text{Im } \pi_i$. The respective dispersion relations, solutions of Eq. (15), must be complex functions as well, i.e., $\omega_\pm = \text{Re } \omega_\pm + i \text{Im } \omega_\pm$. While the real part describes the dispersive phenomenon, the imaginary contribution provides the absorption coefficient $\kappa_\pm \equiv -\text{Im } \omega_\pm$ of mode- \pm photon. This analysis, together with the definition of the vacuum refractive index $n_\pm = |\mathbf{k}|/\text{Re } \omega_\pm$, allows us to establish the relations

$$n_\pm^2 - 1 = \frac{\text{Re } \pi_3 \mp \text{Im } \pi_1}{\text{Re } \omega_\pm^2} \Big|_{k^2=0} \quad \text{and} \quad \kappa_\pm = \frac{\text{Im } \pi_3 \pm \text{Re } \pi_1}{2\text{Re } \omega_\pm} \Big|_{k^2=0}. \quad (16)$$

Observe that the vacuum occupied by the field of the wave [Eq. (3)] is birefringent whenever $\text{Im } \pi_1$ does not vanish identically. We should also mention at this point that the sum of the absorption coefficients coincides with the rate of the photo-production of a $q_\epsilon^+ q_\epsilon^-$ pair in a circularly polarized wave averaged over the photon polarization states [51]. The latter statement is expected since the imaginary part of the polarization tensor is associated with the probability of the pair creation through the optical theorem. Indeed, within the accuracy to the second order with respect to the radiative corrections, the total creation rate of a $q_\epsilon^+ q_\epsilon^-$ pair from a photon with polarization e_ℓ ($\ell = 1, 2$) turns out to be

$$\mathfrak{R}_\ell = \frac{e_\ell^{\mu*} e_\ell^\nu}{\omega} \text{Im } \Pi_{0\mu\nu}(k_1). \quad (17)$$

As long as the photon polarizations are chosen as $e_\pm^\mu = \Lambda_\pm^\mu/2^{1/2}$, the expression above reduces to $\mathfrak{R}_\pm = 2\kappa_\pm$. The corresponding average, on the other hand, turns out to be $\mathfrak{R} = (\mathfrak{R}_+ + \mathfrak{R}_-)/2 = \text{Im } \pi_3/\omega$.³ Detailed calculations of $\text{Im } \pi_3$ may be found in separate papers (see Refs. [51] and [61]) for the various limits to be considered in this work. Because of this fact, in the following we shall be concerned with the determination of the corresponding asymptotic expressions for the remaining quantities contained in Eq. (16).

3. Elastic absorptive properties of the quantum vacuum

The absorption coefficients κ_\pm in Eq. (16) determine the decrement of the probe wave-amplitude due to the production of a pair of MCPs. In order to find an observable effect, we take the incoming probe beam to be a linearly polarized plane wave. Upon entering the region occupied by the external field the probe beam is decomposed into its right and left circular-polarized waves [see Eq. (11)], which initially possess equal amplitudes. As a consequence of the vacuum dichroism, the outgoing probe beam is elliptically polarized [see Fig. (1)] and the following relation for the ellipticity ψ is found

$$\sin(2\psi) = \frac{e^{-2\kappa_+\tau} - e^{-2\kappa_-\tau}}{e^{-2\kappa_+\tau} + e^{-2\kappa_-\tau}}. \quad (18)$$

³Alternatively, the photo-production rate can be calculated from the corresponding transition-amplitude in which the exact nonstationary solution of the Dirac equation for an electron in the field of the wave is considered [47, 48].

Here τ indicates the interacting time. Note that, contrary to the situation where a constant magnetic field drives the dichroism [10, 16, 54], $\psi(\tau)$ is determined here by the damping factors $e^{-\kappa_{\pm}\tau}$ associated with the two propagating modes. The effect is expected to be tiny $\psi \ll 1$ and, consequently, the previous expression can be approached to

$$\psi(\tau) \simeq \frac{1}{2}|\kappa_- - \kappa_+| \tau. \quad (19)$$

We remark that the last formula is a good approximation only when $|\kappa_- - \kappa_+| \tau \ll 1$. Incidentally, Eq. (19) also applies when an optically active crystal is studied [for details see [62] and references therein]. This fact allows then to establish an analogy between our problem and the optics associated with a chiral medium.

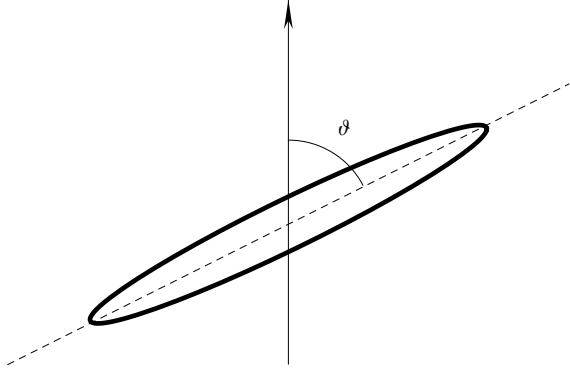


Figure 1: A schematic representation of the optical effects induced on a probe beam after the interaction with a high-intensity circularly polarized laser. The vertical axis must be understood as the direction in which the incoming monochromatic wave is linearly polarized. As a consequence of the interaction with the strong field, the outgoing wave turns out to be elliptically polarized [Eq. (19)] with the principal axis of the ellipse rotated by a small angle ϑ [Eq. (41)].

old value $n_* = 2m_*^2/k\mathcal{X}$. In this context, $m_* \equiv m_\epsilon(1 + \xi_\epsilon^2)^{1/2}$ must be understood as the effective mass which the MCPs acquire due to the field of the wave.

3.1. Two-photon reaction and circular dichroism at $\xi_\epsilon < 1$

Let us start by determining κ_{\pm} [Eq. (16)] as the intense laser parameter $\xi_\epsilon < 1$ and $n_* \leq 1$. Combining the previous conditions we obtain that the results to be derived in this subsection do apply whenever the inequality $\lambda_\epsilon > 2\xi_\epsilon^2$ is fulfilled. In this case, the oscillatory term present in the exponent of Eq. (8) is smaller than the remaining contributions. Consequently, we can ignore it and deal with the following expression

$$\pi_1^{(\frac{1}{2})} \simeq -\frac{4\alpha_\epsilon m_\epsilon^2 \xi_\epsilon^2}{\pi} \int_0^1 dv \int_0^\infty d\rho e^{\frac{-2i\rho(1+\xi_\epsilon^2)}{\lambda_\epsilon(1-v^2)}} \frac{1+v^2}{1-v^2} A_0 \quad (21)$$

where the symmetry of the integrand in the variable v was exploited. Note that for a photon fulfilling the light cone equation, i.e., $k^2 = 0$, the parameter λ_ϵ in Eqs. (8) and (9) is always nonnegative, $\lambda_\epsilon \geq 0$. Because of this fact, we have explicitly taken in Eq. (21) [and also in the following] both $|\lambda_\epsilon| = \lambda_\epsilon$ and $\text{sign}[\lambda_\epsilon] = 1$.

In order to derive an explicit expression of $\text{Re} \pi_1^{(\frac{1}{2})}$, we first integrate by parts the terms containing a factor proportional to $1/\rho^2$. The residue theorem is applied afterwards. The latter step requires an integration contour slightly below the real ρ axis (for details we refer the reader to chapter 3 in [61]). As a consequence, we find

$$\text{Re} \pi_1^{(\frac{1}{2})} \simeq -\frac{\alpha_\epsilon m_\epsilon^2 \xi_\epsilon^2}{2} \int_0^1 dv \Theta \left[1 - \frac{n_*}{(1-v^2)} \right] \frac{1+v^2}{1-v^2} \left\{ \frac{1}{2} - \frac{n_*}{(1-v^2)} \right\} \quad (22)$$

In this context, a purely kinematical analysis proves to be very convenient for forthcoming considerations. To this end we inspect the energy-momentum conservation associated with an absorptive process where n photons of the strong wave are absorbed in addition to a probe photon. In the center-of-mass frame, this is given by $k + n\kappa = q_+ + q_-$ where the four-momentum

$$q_{\pm}^{\mu} \equiv (\varepsilon, \pm\mathbf{q}) = p_{\pm}^{\mu} + \frac{m_\epsilon^2 \xi_\epsilon^2}{2(\mathcal{X} p_{\pm})} \mathcal{X}_{\mu} \quad \text{with} \quad p_{\pm}^2 = m_\epsilon^2$$

is the appropriate translation generator of the vacuum symmetry group in an external field [64]. Consequently, we find the relation $n\kappa\mathcal{X} = 2\varepsilon^2$ with ε being the laser-dressed energy. Here the relative speed between the final particle states turns out to be

$$|\mathbf{v}_{\text{rel}}| = |\mathbf{v}_- - \mathbf{v}_+| = 2v \quad \text{with} \quad v = \left(1 - \frac{n_*}{n} \right)^{1/2}. \quad (20)$$

Eq. (20) reveals that the photo-production of a $q_\epsilon^+ q_\epsilon^-$ pair may take place whenever the number of absorbed photons of the high-intensity laser wave exceeds the thresh-

where $\Theta[x]$ is the unit step function. The latter provides a cut-off from above in the integral contained in Eq. (22). In correspondence, the divergence at $v = 1$ is removed and the variable v can be integrated out without any complications. With these details in mind, we end up with

$$\text{Re } \pi_1^{(\frac{1}{2})} \simeq -\frac{\alpha_\epsilon m_\epsilon^2 \xi_\epsilon^2}{2} \left\{ \ln \left(\frac{1+v}{1-v} \right) - 3v \right\} \Theta[v^2] \quad (23)$$

where $v = (1 - n_*)^{1/2}$ refers to the relative speed where only one photon of the high-intensity laser wave has been absorbed. Accordingly, the photo-production of a pair of MCPs could take place through a two-photon reaction $k + \varkappa \rightarrow q_\epsilon^+ + q_\epsilon^-$. We combine this result with the $\text{Im } \pi_1^{(\frac{1}{2})}$ previously computed in Appendix E of Ref. [61] to express the absorption coefficients [Eq. (16)] of the spinor QED in the following form:

$$\kappa_+^{(\frac{1}{2})} = \frac{\alpha_\epsilon m_\epsilon^2 \xi_\epsilon^2}{4\omega} \left\{ \frac{1-v^4}{2(1+\xi_\epsilon^2)} \ln \left(\frac{1+v}{1-v} \right) + 2v \left(1 - \frac{1-v^2}{2(1+\xi_\epsilon^2)} \right) \right\} \Theta[v^2], \quad (24)$$

$$\kappa_-^{(\frac{1}{2})} = \frac{\alpha_\epsilon m_\epsilon^2 \xi_\epsilon^2}{4\omega} \left\{ \left(2 + \frac{1-v^4}{2(1+\xi_\epsilon^2)} \right) \ln \left(\frac{1+v}{1-v} \right) - 4v \left(1 + \frac{1-v^2}{4(1+\xi_\epsilon^2)} \right) \right\} \Theta[v^2]. \quad (25)$$

Now, the procedure for determining $\text{Re } \pi_1^{(0)}$ shares certain similarities with the previous case. Indeed, it can be read off from Eq. (23) by multiplying the latter by $-1/2$, inserting the coefficient $(1 - v^2)$ in front of the logarithmic function and removing the factor 3 in its last term. On the other hand, the imaginary part of $\pi_3^{(0)}$ has been recently computed in Ref. [51]. With these details in mind, the resulting absorption coefficients [Eq. (16)] associated with scalar QED turn out to be

$$\kappa_+^{(0)} = \frac{\alpha_\epsilon m_\epsilon^2 \xi_\epsilon^2}{8\omega} \left\{ v \frac{1-v^2}{1+\xi_\epsilon^2} + \left[1 - v^2 - \frac{1-v^4}{2(1+\xi_\epsilon^2)} \right] \ln \left(\frac{1+v}{1-v} \right) \right\} \Theta[v^2], \quad (26)$$

$$\kappa_-^{(0)} = \frac{\alpha_\epsilon m_\epsilon^2 \xi_\epsilon^2}{8\omega} \left\{ v \left(2 + \frac{1-v^2}{1+\xi_\epsilon^2} \right) - \left[1 - v^2 + \frac{1-v^4}{2(1+\xi_\epsilon^2)} \right] \ln \left(\frac{1+v}{1-v} \right) \right\} \Theta[v^2]. \quad (27)$$

Note that the difference between the absorption coefficients coincides with $\Delta\kappa \equiv \kappa_+ - \kappa_- = \text{Re } \pi_1/\omega$. This applies whatever be the nature of the virtual particles involved in the loop of the vacuum polarization tensor. The explicit expression for spin- $\frac{1}{2}$ particles is easily read from Eq. (23). On the contrary, when scalar propagators determine the loop, the difference turns out to be

$$\Delta\kappa^{(0)} = \frac{\alpha_\epsilon m_\epsilon^2 \xi_\epsilon^2}{4\omega} \left\{ (1 - v^2) \ln \left(\frac{1+v}{1-v} \right) - v \right\} \Theta[v^2]. \quad (28)$$

Let us consider the situation in which the created particles are ultrarelativistic [$v \sim 1$]. In such a limit, the absorption coefficients above behave like

$$\kappa_+^{(\frac{1}{2})} \approx \frac{\alpha_\epsilon m_\epsilon^2 \xi_\epsilon^2}{2\omega}, \quad \kappa_-^{(\frac{1}{2})} \approx -\frac{\alpha_\epsilon m_\epsilon^2 \xi_\epsilon^2}{2\omega} \left\{ \ln \left(\frac{1-v}{2} \right) + 2 \right\}, \quad \kappa_+^{(0)} \approx \alpha(1-v), \quad \kappa_-^{(0)} \approx \frac{\alpha_\epsilon m_\epsilon^2 \xi_\epsilon^2}{4\omega}. \quad (29)$$

Likewise, the respective differences between the absorption coefficients are given by

$$\Delta\kappa^{(\frac{1}{2})} \approx \frac{\alpha_\epsilon m_\epsilon^2 \xi_\epsilon^2}{2\omega} \left\{ \ln \left(\frac{1-v}{2} \right) + 3 \right\} \quad \text{and} \quad \Delta\kappa^{(0)} \approx -\frac{\alpha_\epsilon m_\epsilon^2 \xi_\epsilon^2}{4\omega}. \quad (30)$$

Next, if the particles are created in the center-of-mass frame almost at rest [$v \sim 0$] we find that

$$\kappa_+^{(\frac{1}{2})} \approx \frac{\alpha_\epsilon m_\epsilon^2 \xi_\epsilon^2}{2\omega} v, \quad \kappa_-^{(\frac{1}{2})} \approx \alpha(v^2), \quad \kappa_+^{(0)} \approx \frac{\alpha_\epsilon m_\epsilon^2 \xi_\epsilon^2}{4\omega} v, \quad \kappa_-^{(0)} \approx \alpha(v^2). \quad (31)$$

These results allow us to approach $\Delta\kappa \approx \kappa_+$ independently of the nature of the created particles. Note, in addition, that the limiting case where $\xi_\epsilon \ll 1$ corresponds to the Born approximation. The respective expressions associated with this limit can be read off from Eqs. (23)-(31) by setting $\xi_\epsilon = 0$ in the effective mass m_* .

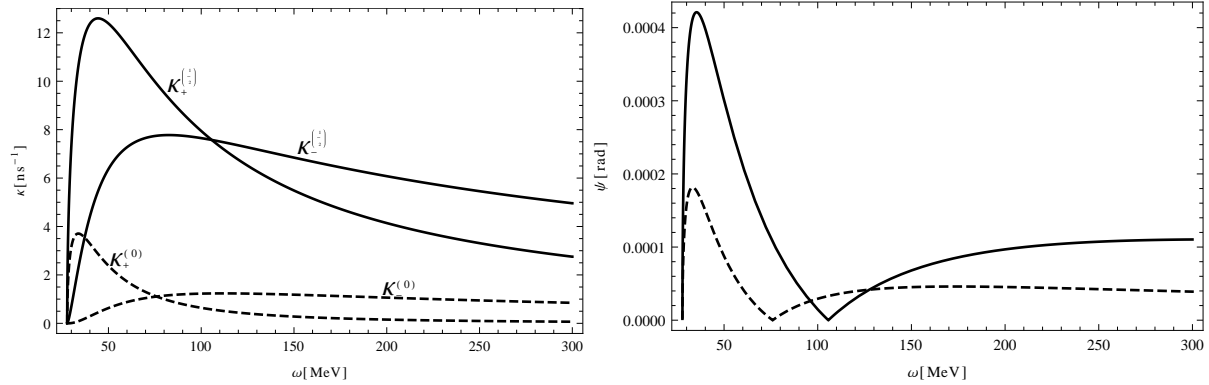


Figure 2: Dependence of the photon absorption coefficients (left) and the ellipticity induced by the vacuum dichroism (right) on the frequency of the probe beam. While the results for spin- $\frac{1}{2}$ particles are represented by solid curves, those corresponding to the scalar situation are given by dashed lines. These results were obtained by considering the parameters given in the text: $\xi = 7.5 \times 10^{-4}$, $\tau \sim 100$ fs, $\varkappa_0 = 9$ keV. The particle charge and mass equal e and m , respectively.

Formula (19), with Eqs. (24)-(31) included, is also of relevance in a pure QED context. This is because it allows us to determine the ellipticity induced by the photo-production of an electron-positron pair. Further analysis in this framework requests to set $\epsilon = 1$ and replace m_ϵ by the electron mass m . It is convenient to clarify that the results obtained in this way are valid for $\xi < 1$ and $\lambda > 1 + \xi^2$ with $\lambda = k\varkappa/(2m^2)$ and $\xi^2 = -e^2 a^2/m^2$. Note besides that, for $\xi \sim 1$ and small values of λ (i.e. $\lambda \sim 2$), next-to-leading order terms with respect to ξ^2/λ could become relevant. We assume a strong laser field with photon energy $\varkappa_0 = 9$ keV, intensity parameter $\xi = 7.5 \times 10^{-4}$ and temporal length $\tau \sim 100$ fs. For this choice, which is inspired by the x-ray free-electron laser facilities (XFEL) currently under construction at DESY (Hamburg, Germany) and SLAC (Stanford, USA), the first Born approximation can be used. With this set of parameters in mind, the photo-production of an electron-positron pair takes place if the probe beam has a frequency $\omega \geq 27.8$ MeV, assuming a head-on collision geometry. When Dirac particles are created, the induced ellipticity is maximized at $\omega \approx 35.3$ MeV. For further information, we refer the reader to Fig. (2), where the dependence of ψ with respect to ω is displayed.

3.2. Extinction of the vacuum dichroism in the limit $\xi_\epsilon \gg 1$

We wish to find out the leading order terms of the photon absorption coefficients κ_\pm [Eq. (16)] as $\xi_\epsilon \gg 1$. In this case, the photo-production rate of a $q_\epsilon^+ q_\epsilon^-$ pair is independent of the frequency of the external laser beam \varkappa_0 and coincides with the rate arising in the constant crossed field configuration [51]. To find the corresponding difference between the absorption coefficients it is convenient to carry out the change of variable $u = (1 - v^2)^{-1}$ in Eq. (8). This leads to express

$$\Delta\kappa^{(\frac{1}{2})}(\lambda_\epsilon, \xi_\epsilon) = \kappa_+^{(\frac{1}{2})} - \kappa_-^{(\frac{1}{2})} = \frac{\text{Re } \pi_1}{\omega} = -\frac{2\alpha_\epsilon m_\epsilon^2 \xi_\epsilon^2}{\pi\omega} \int_1^\infty \frac{du(2u-1)}{2u\sqrt{u(u-1)}} \int_{-\infty}^\infty d\rho A_0 \cos[2u\eta] \quad (32)$$

where the abbreviation $\eta = \frac{\rho}{\lambda_\epsilon} [1 + 2\xi_\epsilon^2 A]$ has been introduced. Note that, although the resulting integrand is a singular function at $u = 1$, the integral over this variable does not diverge around this value. Besides, since the integrand decreases as $\sim 1/u^2$ at $u \rightarrow \infty$ its main contribution to Eq. (32) comes from the region $u \sim 1$. Regarding the integration over the remaining variable, here the integrand falls off as $\rho \rightarrow \pm\infty$ and is, in addition, a regular function in ρ . The experience gained in the calculation of similar integrals (see, for instance, Refs. [51] and [52]) indicates that the asymptotic behavior of Eq. (32) as $\xi_\epsilon \gg 1$ can be determined by splitting the integration domain into three regions:

$$\int_{-\infty}^\infty d\rho \dots = \int_{-\infty}^{-\rho_0} d\rho \dots + \int_{-\rho_0}^{\rho_0} d\rho \dots + \int_{\rho_0}^\infty d\rho \dots \quad (33)$$

where ρ_0 denotes a positive dimensionless parameter which fulfills the conditions

$$\xi_\epsilon^{-1} \ll \rho_0 \ll 1 \quad \text{and} \quad (\lambda_\epsilon/\xi_\epsilon^2)^{1/3} \ll \rho_0. \quad (34)$$

The second condition implies that the process under consideration requires a high number of photons which are absorbed from the strong field of the wave, i.e., $n \geq n_* \approx \xi_\epsilon^2/\lambda_\epsilon \gg 1$ [multi-photon reaction]. For further convenience we denote the integration regions on the right-hand side of Eq. (33) from left to right as *lower region*, *inner region* and *upper region*, respectively. Observe that $|\rho| \leq \rho_0 \ll 1$ within the inner integration region. In correspondence, we Taylor expand η and, separately, the remaining part of the integrand. Next, the change of variable $s = \rho\xi_\epsilon$ is performed in the resulting integral and also in those defined over the lower and upper regions. Afterwards, the integration limit $\rho_0\xi_\epsilon$ is extended to infinity. This last step provides no contribution from the integral associated with the lower and upper regions and yields to approach the total integral over ρ by

$$\int_{-\infty}^{\infty} d\rho \dots \approx \frac{1}{6\xi_\epsilon^3} \int_{-\infty}^{\infty} ds s^2 \cos\left[\frac{2u}{\lambda_\epsilon\xi_\epsilon} \left(s + \frac{s^3}{3}\right)\right]. \quad (35)$$

Some comments are in order. First of all, the last approximation turns out to be accurate up to terms that decrease exponentially, like $\sim (\rho_0\xi_\epsilon)^{-1} \exp\left[-\frac{2u}{3\lambda_\epsilon\xi_\epsilon}(\rho_0\xi_\epsilon)^3\right]$ and faster. Moreover, once the following representation of the Macdonald function is considered:⁴

$$\int_{-\infty}^{\infty} dy y^2 \cos(by + ay^3) = -\frac{2}{9} \frac{b^{3/2}}{a^{3/2}} K_{1/3}\left(\frac{2}{3\sqrt{3}} \frac{b^{3/2}}{a^{1/2}}\right), \quad (36)$$

Eq. (32) acquires the following structure:

$$\Delta\kappa^{(\frac{1}{2})} \simeq \frac{\alpha m_\epsilon^2}{3\sqrt{3}\pi\omega\xi_\epsilon} \int_1^{\infty} \frac{du}{u\sqrt{u(u-1)}} K_{1/3}\left(\frac{4u}{3\zeta_\epsilon}\right) (2u-1). \quad (37)$$

The situation in which spin-0 particles are created does not differ too much from the previous case. Hence, the leading asymptotic behavior of $\Delta\kappa^{(0)}$ as $\xi_\epsilon \gg 1$ turns out to be

$$\Delta\kappa^{(0)} \simeq \frac{\alpha m_\epsilon^2}{6\sqrt{3}\pi\omega\xi_\epsilon} \int_1^{\infty} \frac{du}{u\sqrt{u(u-1)}} K_{1/3}\left(\frac{4u}{3\zeta_\epsilon}\right). \quad (38)$$

The set of Eqs. (37) and (38) involves the abbreviation $\zeta_\epsilon \equiv \lambda_\epsilon\xi_\epsilon = \frac{\epsilon\omega m_\epsilon^2}{2m_\epsilon^3} \frac{E}{E_c} (1 - \hat{\mathbf{n}} \cdot \hat{\boldsymbol{\varkappa}})$ with $E_c = m^2/e = 1.3 \times 10^{16}$ V/cm the critical electric field of QED. Here $\hat{\mathbf{n}} = \mathbf{k}/|\mathbf{k}|$ and $\hat{\boldsymbol{\varkappa}} = \boldsymbol{\varkappa}/|\boldsymbol{\varkappa}|$ denote the propagation directions of the probe and the strong laser field, respectively. Note that Eqs. (37) and (38) are structurally similar to the respective expressions of the photo-production rates \mathfrak{R} [61, 51]. It is noticeable, however, that in contrast to the latter, they are suppressed by a factor $\sim 1/\xi_\epsilon$ which, in addition, depends on the frequency of the high-intensity laser. Hence, $\Delta\kappa$ can be understood as a term which is sensitive to the properties of the strong wave. This kind of dependence also emerges in \mathfrak{R} when corrections, next-to-leading order, are taken into account [61]. In order to evaluate the role of $\Delta\kappa$ within the absorption coefficients, it is convenient to express them as $\kappa_\pm = (\mathfrak{R} \pm \Delta\kappa)/2$. This makes evident that $\Delta\kappa$ acts as a small correction, too. As a consequence, the production of pairs is equally plausible in either of the two propagating modes, leading to approach $\kappa_\pm \approx \mathfrak{R}/2 \pm o(\xi_\epsilon^{-1})$. Here we do not present any picture of the rates \mathfrak{R} because a numerical assessment of this issue has been recently carried out in Ref. [63]. Instead, we just emphasize that, with the increasing of the intensity of the strong background laser, the vacuum becomes less and less dichroic to a linearly polarized probe beam, contrary to what occurs in a vacuum polarized by a constant crossed field.

This different behavior is closely connected to the invariance properties of each problem. In a constant crossed field configuration, the vacuum behaves like a biaxial medium and its symmetry is no longer described by Poincaré's group. Instead, a subgroup of it maps the actual invariance of the Minkowski space occupied by the external field. It is the vacuum polarization tensor $\Pi_{\mu\nu}$ which incorporates this anisotropy into the gauge sector of QED [Eq. (1)]. Therefore, the problem associated with the photon propagation is no longer degenerated in the energy since the physical degrees of freedom are described by birefringent states [for details we refer the reader to Ref. [26]]. Consequently, the helicity is no longer necessary for labeling the one-particle state. The situation is quite different in the field of a circularly

⁴Derivation of Eq. (36) requires to combine Eqs. (3.695.1-2) in Ref. [68] and differentiate the resulting expression twice with respect to b .

polarized monochromatic plane wave. Here the quantum vacuum behaves like an anisotropic chiral medium and is invariant with respect to the following operation: translation by an arbitrary vector β^{μ} followed by a spatial rotation about the direction of the wave propagation $\hat{\mathbf{x}}$ of the field by an angle $\simeq \beta$ [45, 64]. Clearly, in the limit $\xi_{\epsilon} \gg 1$ the independence of the high-intensity laser frequency renders the problem quasi-static with respect to the external field. This means that, in the interaction, the probe beam does not perceive the rotation of the strong field of the wave and the external field seems to be—in average—isotropically distributed in the vacuum. This “new” isotropy of the spacetime causes the photon propagation problem to be quasi-degenerated in the energy. Hence, the physical modes that emerge from the interaction can be described approximately by monochromatic waves with opposite helicity.

It is convenient to remark that the suppression of $\Delta\kappa$ cannot be compensated by the dependence on ξ_{ϵ} present in the Macdonald functions of Eqs. (37) and (38). This becomes manifest as soon as the main asymptotic behaviors of $\Delta\kappa$ are taken into account. In order to show the latter we consider first the situation in which $\zeta_{\epsilon} \gg 1$. Consistency with our original condition ($\xi_{\epsilon} \gg 1$) requires to restrict the parameter λ_{ϵ} to values with $\lambda_{\epsilon} \gg 1/\xi_{\epsilon}$. Applying the small-argument behavior of the functions $K_{\nu}(z) \sim \frac{\Gamma(\nu)}{2} \left(\frac{z}{2}\right)^{\nu}$ [68] we find

$$\Delta\kappa^{(\frac{1}{2})} \approx \frac{\alpha_{\epsilon} m_{\epsilon}^2 \lambda_{\epsilon}}{3 \sqrt{3} \pi \omega \zeta_{\epsilon}^{2/3}} \left(\frac{2}{3}\right)^{2/3} \frac{\Gamma^2\left(\frac{1}{3}\right)}{\Gamma\left(\frac{11}{6}\right)}, \quad \Delta\kappa^{(0)} \approx \frac{1}{8} \Delta\kappa^{(\frac{1}{2})}, \quad (39)$$

where $\Gamma(x)$ denotes the Gamma function. So, in the limit under consideration the difference between the absorption coefficients decreases as $\Delta\kappa \sim \xi_{\epsilon}^{-2/3}$. Meanwhile, the leading order term in \mathfrak{R} scales as $\sim \xi_{\epsilon}^{2/3}$, which turns out to be $\xi_{\epsilon}^{4/3}$ greater than $\Delta\kappa$. Let us now turn our attention to the case where $\zeta_{\epsilon} \ll 1$. The latter is in correspondence with the conditions $\xi_{\epsilon} \gg 1$ and $\lambda_{\epsilon} \ll \xi_{\epsilon}^{-1}$, in which case one is able to exploit the large argument behavior of the Macdonald function, i.e., $K_{\nu}(z) \sim \sqrt{\frac{\pi}{2z}} e^{-z}$ [68]. With this expansion in mind, the variable u can be integrated out. As a consequence

$$\Delta\kappa^{(\frac{1}{2})} \approx \frac{\alpha_{\epsilon} m_{\epsilon}^2 \lambda_{\epsilon}}{12 \omega} \sqrt{\frac{3}{2}} e^{-\frac{4}{3\zeta_{\epsilon}}} \quad \text{and} \quad \Delta\kappa^{(0)} \approx \frac{1}{2} \Delta\kappa^{(\frac{1}{2})}. \quad (40)$$

In this context, we also find that the leading expressions of \mathfrak{R} exceed by a factor $\simeq \xi_{\epsilon}$ the corresponding expression of $\Delta\kappa$. Clearly, owing to the extinction of the vacuum dichroism the ellipticity [Eq. (19)] is difficult to detect. In correspondence, another kind of observable is needed to probe the effects induced by the vacuum polarization.

4. Elastic dispersive properties of the nonlinear vacuum

The QED vacuum—polarized by an external field—behaves like a material medium, in which light propagation is modified. Besides the dichroic effects, the vacuum birefringence is predicted to take place: during the interaction with the strong field of the wave, the helicity components of the probe beam accumulate a relative difference of the phase. This fact is closely connected with the vacuum refraction indices [Eq. (16)]. In correspondence, the incoming linearly polarized probe beam undergoes a tiny rotation [see Fig. (1)] with respect to the initial polarization plane. This constitutes another observable which is looked for in the polarimetric experiments. In the context under consideration, the rotation angle of the polarization axis reads

$$\vartheta(\tau) = \frac{1}{2} \frac{n_{+} - n_{-}}{n_{+} n_{-}} \omega \tau. \quad (41)$$

Whenever the dispersive effects are very small, i.e., $n_{\pm} \approx 1$, the denominator of Eq. (41) can be taken as unity. The resulting expression resembles the rotation angle that a probe beam undergoes after traversing a chiral medium. In the following, we study the regions where Eq. (41) could be of interest in the search of MCPs but also in a pure QED context.

4.1. Photon propagation at $\xi_{\epsilon} \lesssim 1$ and $\lambda_{\epsilon} \ll 1$

The kinematic domain where no absorption of probe photons occurs defines the transparency region. Here the dispersion relations are real functions which remain below the first pair creation threshold, $1 < n_{*}$. However, in the

following we will restrict ourselves to $1 \ll n_*$ where the determination of the vacuum refraction indices [Eq. (16)] is substantially simplified. To show this, let us undertake the calculation of an alternative representation⁵ of $\pi_3^{(0)}$

$$\pi_3^{(0)} = -\frac{\alpha_\epsilon m_\epsilon^2 \xi_\epsilon^2}{\pi} \int_1^\infty \frac{du}{2u \sqrt{u(u-1)}} \int_0^\infty \frac{d\rho}{\rho} e^{-2iu\eta} \left\{ \sin^2(\rho) - \frac{8i}{\lambda_\epsilon} u(u-1) \rho A_0 \right\}. \quad (42)$$

The expression above involves A_0 [Eq. (10)] and η which is defined below Eq. (32). Whenever $\xi_\epsilon \lesssim 1$ the oscillating term in η becomes smaller than the remaining contribution so that one can approach $\eta \approx \rho/\lambda_\epsilon$. In this limit, the main contribution to the integral over ρ comes from the region where $\rho \sim \lambda_\epsilon \ll 1$. Hence, we can Taylor expand the integrand and obtain

$$\int_0^\infty \frac{d\rho}{\rho} \dots \simeq \int_0^\infty d\rho \rho e^{-\frac{2iu\rho}{\lambda_\epsilon}} \left(1 - \frac{4iu(u-1)}{3\lambda_\epsilon} \rho \right). \quad (43)$$

Because of the absence of poles, one can use Cauchy's theorem to rotate the integration contour by $\rho \rightarrow -i\rho$. In correspondence, the variable ρ can be integrated out and one ends up with

$$\pi_3^{(0)} \simeq \frac{\alpha_\epsilon m_\epsilon^2 \zeta_\epsilon^2}{24\pi} \int_1^\infty \frac{du (7-4u)}{u^3 \sqrt{u(u-1)}} = \frac{4}{45} \frac{\alpha_\epsilon}{\pi} m_\epsilon^2 \zeta_\epsilon^2, \quad (44)$$

with $\zeta_\epsilon = \lambda_\epsilon \xi_\epsilon$ as before. Besides, following a similar procedure, we are able to find that $\pi_1^{(0)} \simeq 4i\alpha_\epsilon m_\epsilon^2 \zeta_\epsilon^2 \lambda_\epsilon / (105\pi)$, which turns out to be smaller than $\pi_3^{(0)}$ by a factor $\sim \lambda_\epsilon$. Hence, for both helicity modes of the probe beam, the refraction index [Eq. (16)] is well approached by

$$n^{(0)} \simeq 1 + \frac{2}{45} \frac{\alpha_\epsilon}{\pi} \frac{m_\epsilon^2}{\omega^2} \zeta_\epsilon^2, \quad n^{(\frac{1}{2})} \simeq 1 + \frac{11}{45} \frac{\alpha_\epsilon}{\pi} \frac{m_\epsilon^2}{\omega^2} \zeta_\epsilon^2. \quad (45)$$

The case where the polarization tensor is determined from spin- $\frac{1}{2}$ propagators has been quoted from Ref. [44]. According to these expressions, the vacuum in the field of the wave behaves—with an accuracy up to terms $\sim \lambda_\epsilon$ —as a nonbirefringent medium. Finally, we point out that in the limits under consideration both refraction indices can be obtained from the respective Euler-Heisenberg Lagrangian. Considerations of this nature have been carried out in Ref. [65, 66] (see also [67]).

4.2. Chiral birefringence at $\xi_\epsilon < 1$ and $\lambda_\epsilon \gtrsim 1$

The vacuum of virtual $q_\epsilon^+ q_\epsilon^-$ pairs manifests a chiral birefringence when the conditions $\xi_\epsilon < 1$ and $n_* \lesssim 1$ are simultaneously fulfilled. To show this, we start by considering the case where the polarization tensor is determined from spinor QED. In such a situation, the real and imaginary parts of the form factors involved in the refraction indices [Eq. (16)] can be approached by

$$\text{Re } \pi_3^{(\frac{1}{2})} \simeq \frac{2\alpha_\epsilon m_\epsilon^2 \xi_\epsilon^2}{\pi} \int_0^1 dv \int_0^\infty d\rho \frac{\sin^2(\rho)}{\rho} \left\{ \frac{n_*}{(1+\xi_\epsilon^2)(1-v^2)\rho} \sin\left(\frac{2n_*\rho}{1-v^2}\right) - \frac{1+v^2}{1-v^2} \cos\left(\frac{2n_*\rho}{1-v^2}\right) \right\}, \quad (46)$$

$$\text{Im } \pi_1^{(\frac{1}{2})} \simeq \frac{2\alpha_\epsilon m_\epsilon^2 \xi_\epsilon^2}{\pi} \int_0^1 dv \int_0^\infty d\rho \frac{1+v^2}{1-v^2} \left\{ \frac{\sin^2(\rho)}{\rho^2} - \frac{\sin(2\rho)}{2\rho} \right\} \sin\left(\frac{2n_*\rho}{1-v^2}\right) \quad (47)$$

where the oscillatory term present in the exponent of Eq. (8) has been neglected. Consequently, we will be working within the same accuracy limits described in Sec. 3.1. The integral over ρ can, then, be done with the help of the following identities:

$$\int_0^\infty \frac{dx}{x^2} \sin^2(x) \sin(2cx) = \frac{1}{2} (1+c) \ln(1+c) - c \ln(c) - \frac{1}{2} (1-c) \ln|1-c| \quad \text{for } c > 0,$$

$$\int_0^\infty \frac{dx}{x} \sin(2x) \sin(2cx) = \frac{1}{4} \ln\left(\frac{1+c}{1-c}\right)^2 \quad \text{for } c \neq 1, \quad (48)$$

$$\int_0^\infty \frac{dx}{x} \sin^2(x) \cos(2cx) = \frac{1}{4} \ln\left[\frac{(1+c)|1-c|}{c^2}\right] \quad \text{for } c > 0 \quad \text{and } c \neq 1.$$

⁵A detailed explanation about the operation needed to obtain Eq. (42) can be found in Eq. (27) of Ref. [51].

It is worth mentioning at this point that the expression contained in the first line of Eq. (48), as well as the formula in the second line, results from an appropriated particularization of Eqs. (3.763.3) and (3.741.1) of Ref. [68], respectively. The remaining relation is just the derivative of the expression of the first line. With these details in mind, one finds that

$$\begin{aligned} \text{Re } \pi_3^{(\frac{1}{2})} \simeq & -\frac{\alpha_\epsilon m_\epsilon^2 \xi_\epsilon^2}{\pi} \int_0^1 dv \left\{ -\frac{2n_*}{(1+\xi_\epsilon^2)(1-v^2)} \ln \left[\frac{1-v^2+n_*}{|1-v^2-n_*|} \right]^{1/2} + \left(\frac{2n_*^2}{(1+\xi_\epsilon^2)(1-v^2)^2} - \frac{1+v^2}{1-v^2} \right) \right. \\ & \left. \times \ln \left[\frac{n_*}{|(1-v^2)^2 - n_*^2|^{1/2}} \right] \right\}, \end{aligned} \quad (49)$$

$$\text{Im } \pi_1^{(\frac{1}{2})} \simeq \frac{\alpha_\epsilon m_\epsilon^2 \xi_\epsilon^2}{\pi} \int_0^1 dv \frac{1+v^2}{1-v^2} \left\{ \ln \left[\frac{1-v^2+n_*}{|1-v^2-n_*|} \right]^{1/2} - \frac{2n_*}{1-v^2} \ln \left[\frac{n_*}{|(1-v^2)^2 - n_*^2|^{1/2}} \right] \right\}. \quad (50)$$

The corresponding quantities coming from scalar QED can be read off from Eqs. (49) and (50). To do this, one has to replace $(1+v^2)/(1-v^2) \rightarrow 1$ and multiply the right-hand side of these expressions by a factor 1/2, afterwards. Additionally, the derivation of $\text{Re } \pi_3^{(0)}$ requires to change the signs of the first two terms coming from Eq. (49). Observe that an exact evaluation of the integral over v is quite difficult to perform. However, when our calculations are particularized with the QED parameters, i.e., $\epsilon = 1$ and $m_\epsilon \rightarrow m$, it can be integrated numerically without too much efforts. The resulting corrections to the vacuum refraction indices are displayed in Fig. (3). These results were obtained by setting the external field parameters to the envisaged XFEL facility.

Now, the dependence on n_* allows us to obtain—as in Sec. 3.1—analytical expressions of the vacuum refraction indices. To this end, we insert Eqs. (49) and (50) into Eq. (16). The presence of the function $|1-v^2-n_*|$ is then used to write the resulting expression as follows:

$$n_\pm^{(\frac{1}{2})} \simeq 1 + \frac{\alpha_\epsilon m_\epsilon^2 \xi_\epsilon^2}{2\pi\omega^2} \left\{ \int_0^{\sqrt{1-n_*}} dv (\dots \mp \dots) + \int_{\sqrt{1-n_*}}^1 dv (\dots \mp \dots) \right\}. \quad (51)$$

The respective integrands turn out to be free of functions involving the absolute value and contain logarithmic divergences at $v = \sqrt{1-n_*}$. In contrast to the first one, the last integrand in Eq. (51) has an additional divergence at $v = 1$. Clearly, whenever $n_* \leq 1$, both refraction indices are real, a fact which agrees with the considerations used in the derivation of Eq. (16). Note that, in the region under consideration, the photo-production of a $q_\epsilon^+ q_\epsilon^-$ -pair could take place [see Sec. 3.1]. Therefore, the refraction indices in Eq. (51) describe the dispersive properties of those photons that—having the proper energies—do not take part in the two-photon reaction. It is precisely in a vicinity of the corresponding threshold [$n_* \simeq 1$] where the chiral birefringence effect turns out to be maximized. This is manifest within the QED context [see Fig. (3)]. Hence, finding expressions which describe the situation in this particular limit is also of interest. To this end, we set $n_* = 1$ and compute the relevant integral by using MATHEMATICA code. As a consequence,

$$n_\pm^{(\frac{1}{2})} \Big|_{n_*=1} \approx 1 + \frac{\alpha_\epsilon m_\epsilon^2 \xi_\epsilon^2}{2\pi\omega^2} \left(0.9 + \frac{1.2}{1+\xi_\epsilon^2} \pm 0.5 \right), \quad n_\pm^{(0)} \Big|_{n_*=1} \approx 1 + \frac{\alpha_\epsilon m_\epsilon^2 \xi_\epsilon^2}{4\pi\omega^2} \left(0.8 - \frac{1.2}{1+\xi_\epsilon^2} \pm 0.4 \right) \quad (52)$$

where the outcome resulting from scalar QED has been included. The explicit expression of the rotation angle follows by inserting Eq. (52) into Eq. (19). Consequently,

$$\vartheta^{(\frac{1}{2})}(\tau) \Big|_{n_*=1} \approx \frac{\alpha_\epsilon m_\epsilon^2 \xi_\epsilon^2}{4\pi\omega} \tau \quad \text{and} \quad \vartheta^{(0)}(\tau) \Big|_{n_*=1} \approx 0.4 \vartheta^{(\frac{1}{2})}(\tau) \Big|_{n_*=1}. \quad (53)$$

We remark that, in both cases, the rotation angle enhances when the frequency of the probe beam is small and the product $\xi_\epsilon^2 \tau$ becomes large. It is also convenient to emphasize that Eq. (53) is applicable only when $m_\epsilon = [(\varkappa k)/2]^{1/2}$. As last remark of this subsection, we point out that the expressions associated with the first Born [$\xi_\epsilon \ll 1$] approximation can be obtained from Eq. (52) just by setting $\xi_\epsilon^2 = 0$ in the fraction contained within the brackets.

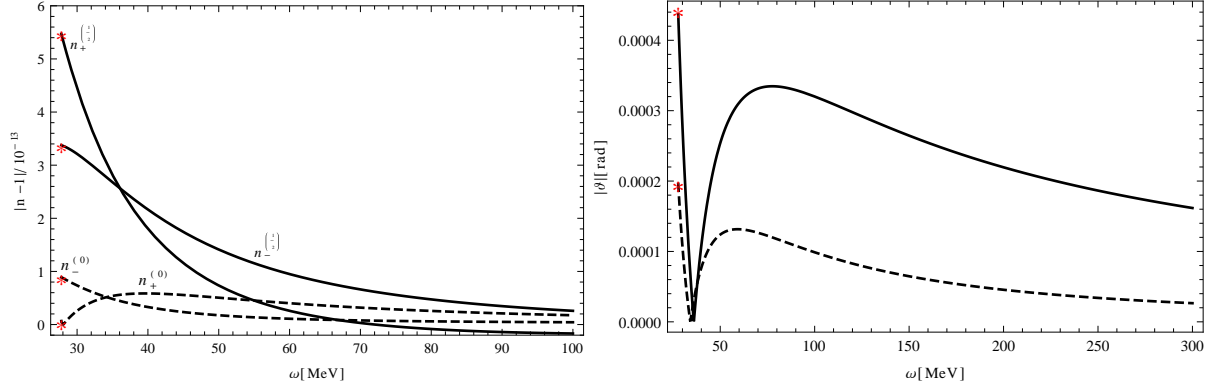


Figure 3: Correction to the vacuum refraction indices (left) and the rotation of the polarization plane induced by the vacuum birefringence (right) in terms of the frequency of the probe laser. While the result for spin- $\frac{1}{2}$ particles are represented by solid curves, those corresponding to the scalar situation are given by dashed lines. These results were obtained by considering the envisaged XFEL parameters: $\xi = 7.5 \times 10^{-4}$, $\tau \sim 100$ fs, $\varkappa_0 = 9$ keV. The particle charge and mass equal e and m , respectively.

4.3. Large asymptotic behavior of the vacuum refraction indices at $\xi_\epsilon \gg 1$

Our aim in this subsection is to determine the asymptotic behavior of those quantities associated with the vacuum birefringence as $\xi_\epsilon \gg 1$. The problem under consideration is quite analogous to the one analyzed in Sec. 3.2, so that the line of reasoning will be similar. However, some differences will emerge in the course of the calculations. These differences come out from the nature of $\text{Re } \pi_1$ and $\text{Im } \pi_3$ involved in Eq. (16). Let us undertake, in first instance, the computation of the difference between the vacuum refraction indices. Within the framework of spinor QED, and with the help of Eqs. (16) and (8)-(10), the latter turns out to be

$$\Delta n^{(\frac{1}{2})}(\lambda_\epsilon, \xi_\epsilon) = n_+^{(\frac{1}{2})} - n_-^{(\frac{1}{2})} \simeq -\frac{\text{Im } \pi_1^{(\frac{1}{2})}}{\omega^2} \simeq -\frac{4\alpha_\epsilon m_\epsilon^2 \xi_\epsilon^2}{\pi \omega^2} \int_1^\infty \frac{du(2u-1)}{2u\sqrt{u(u-1)}} \int_0^\infty d\rho A_0 \sin(2u\eta). \quad (54)$$

We follow the premise of dividing the ρ -interval into two domains: from 0 to ρ_0 and from ρ_0 to ∞ with $\xi_\epsilon^{-1} \ll \rho_0 \ll 1$. Once this step has been carried out, we are allowed to Taylor expand $A_0 \approx \rho^2/6$ and $\eta = \frac{\rho}{\lambda_\epsilon} [1 + \xi_\epsilon A] \approx \frac{1}{\zeta_\epsilon} \left[\rho \xi_\epsilon + \frac{(\rho \xi_\epsilon)^3}{3} \right]$ separately in the interval where $\rho \in [0, \rho_0]$. In correspondence, Eq. (54) approaches to

$$\Delta n^{(\frac{1}{2})} \simeq -\frac{\alpha_\epsilon m_\epsilon^2}{3\pi \omega^2 \xi_\epsilon} \int_1^\infty \frac{du(2u-1)}{u\sqrt{u(u-1)}} \int_0^\infty ds s^2 \sin \left[\frac{2u}{\zeta_\epsilon} \left(s + \frac{s^3}{3} \right) \right]. \quad (55)$$

The derivation of this equation requires to perform the change of variable $\rho \xi_\epsilon \rightarrow s$ and to extend the resulting integration limit to infinity [$\rho_0 \xi_\epsilon \rightarrow \infty$]. We remark that Eq. (55) turns out to be a good approximation only if the exponential $\sim \exp \left[-\frac{2u}{3\zeta_\epsilon} (\rho_0 \xi_\epsilon)^3 \right]$ falls off sufficiently fast as $\rho_0 \xi_\epsilon \gg 1$. Of course, the latter condition is satisfied whenever the exponent is very large, in which case the complementary restriction [Eq. (34)] $1 \gg \rho_0 \gg (\lambda_\epsilon / \xi_\epsilon^2)^{1/3}$ is found. Formally, it should appear an additional dependence on the variable u . Nonetheless, we have set $u \sim 1$ because the vicinity of this value provides the main contribution of the u -integral.

Now, we perform the change of variable $(2u/\zeta_\epsilon)^{1/3} s \rightarrow y$ and express the integral over s in terms of the second derivative of Scorer's function [69]⁶:

$$\int_0^\infty ds \dots = \frac{\zeta_\epsilon \pi}{2u} \text{Gi}''(z) \quad \text{with} \quad \text{Gi}(z) = \frac{1}{\pi} \int_0^\infty dy \sin \left(zy + \frac{y^3}{3} \right) \quad \text{and} \quad z \equiv \left(\frac{2u}{\zeta_\epsilon} \right)^{2/3}. \quad (56)$$

⁶The name of this function varies in the literature. A summary of its properties can be found on page 448 of Ref. [70]. Another compact recap is given in Appendix E of Ref. [71] with the name of Hardy's function $\Upsilon(z)$. In [72], the name Upsilon function is used. A relation between both notations can be established according to $\Upsilon(z) = \pi \text{Gi}(z)$.

We insert this expression into Eq. (55) and use the differential equation $\text{Gi}''(z) - z\text{Gi}(z) = -\pi^{-1}$ afterwards. With these steps in mind, the differences between the vacuum refraction indices turn out to be

$$\Delta n^{(\frac{1}{2})} \simeq -\frac{4\alpha_\epsilon m_\epsilon^2 \lambda_\epsilon}{9\pi\omega^2} + \frac{2^{2/3}\alpha_\epsilon m_\epsilon^2 \lambda_\epsilon}{6\omega^2 \zeta_\epsilon^{2/3}} \int_1^\infty \frac{du(2u-1)}{u^{4/3} \sqrt{u(u-1)}} \text{Gi}(z), \quad (57)$$

$$\Delta n^{(0)} \simeq -\frac{2\alpha_\epsilon m_\epsilon^2 \lambda_\epsilon}{9\pi\omega^2} + \frac{2^{2/3}\alpha_\epsilon m_\epsilon^2 \lambda_\epsilon}{12\omega^2 \zeta_\epsilon^{2/3}} \int_1^\infty \frac{du}{u^{4/3} \sqrt{u(u-1)}} \text{Gi}(z). \quad (58)$$

Note that Eqs. (57) and (58) depend—as for $\Delta\kappa$ in Sec. 3.2—on the frequency of the high-intensity laser, a fact which does not find a counterpart in the constant crossed field approach.

It is interesting to proceed by restricting the parameter ζ_ϵ to some asymptotic limits of interest. We start with the situation in which $\zeta_\epsilon \gg 1$ [corresponding to $\lambda_\epsilon \gg 1/\xi_\epsilon$ with $\xi_\epsilon \gg 1$]. Considering the appropriate expansion of Scorer's function at $z \ll 1$, i.e., $\text{Gi}(z) \sim \frac{1}{2\pi^{3/3}} \Gamma\left(\frac{1}{3}\right) + \frac{1}{2\pi^{3/3}} \Gamma\left(\frac{2}{3}\right)z$, one obtains

$$\Delta n^{(\frac{1}{2})} \simeq \frac{4\alpha_\epsilon m_\epsilon^2 \lambda_\epsilon}{9\pi\omega^2} + \frac{\sqrt{3}}{3\omega} \Delta\kappa^{(\frac{1}{2})} \quad \text{and} \quad \Delta n^{(0)} \simeq \frac{2\alpha_\epsilon m_\epsilon^2 \lambda_\epsilon}{9\pi\omega^2} + \frac{\sqrt{3}}{2\omega} \Delta\kappa^{(0)}. \quad (59)$$

We point out that the quantity $\Delta\kappa$ can be found in Eq. (39). Since it is suppressed by a factor $\sim 1/\xi_\epsilon$ one can ignore its contribution and just deal with the leading order terms. The latter are independent of the parameter ξ_ϵ and maximized when the collision between the probe and the external wave is head-on. We should also mention that, although the leading term is independent of the mass of the particle, it applies for those values with $m_\epsilon \ll [\epsilon(kz\tau)m/2]^{1/3}$. Moreover, the rotation angle, which comes out of combining the expression for $\Delta n^{(\frac{1}{2})}$ with Eq. (41), is independent of the frequency of the probe beam. Considering the configuration in which both lasers counterpropagate, we find

$$\vartheta^{(\frac{1}{2})}(\tau) = \frac{2\alpha}{9\pi} \epsilon^2 \varkappa_0 \tau \quad (60)$$

where τ is the interacting time and $\alpha = 1/137$ the QED fine structure constant. Observe that a comparison with the rotation angle coming out from the scalar case leads to write $\vartheta^{(\frac{1}{2})} \approx 2\vartheta^{(0)}$.

The situation is slightly different in the case where $\zeta_\epsilon \ll 1$. This condition restricts $\lambda_\epsilon \ll 1$ with $\xi_\epsilon \gg 1$. In this context, the large asymptotic behavior of Scorer's function applies, i.e., $\text{Gi}(z) \sim \frac{1}{\pi z} + \frac{2}{\pi z^2}$. Consequently, we can develop the integral over u and find that

$$\Delta n^{(\frac{1}{2})} \simeq \frac{32\alpha_\epsilon m_\epsilon^2 \zeta_\epsilon^2}{315\pi \omega^2 \xi_\epsilon} \quad \text{and} \quad \Delta n^{(0)} \simeq \frac{n^{(\frac{1}{2})}}{4}. \quad (61)$$

Accordingly, a suppression $\sim \xi_\epsilon^{-1}$ of Δn occurs. Therefore, under the aforementioned circumstance, the nonlinear vacuum of QED seems to behave as a material in which dichroism [Eqs. (39) and (40)] and birefringence are practically absent. We will shortly retake this point again.

We want to conclude this section by determining the expression of the vacuum refraction indices. According to Eq. (16) and (54), it can be written as

$$n_\pm^2 - 1 = \frac{\text{Re } \pi_3}{\omega^2} \pm \Delta n. \quad (62)$$

We have already determined the leading behavior of Δn as $\xi_\epsilon \gg 1$. So, our goal now is to compute the isotropic contribution $\sim \text{Re } \pi_3/\omega^2$. To undertake the calculation, we first integrate by parts those terms of the integrand Ω_3 [Eq. (9)] proportional to $\sim (1 - e^y)$. This step allows us to express the contribution resulting from spinor QED in the following form: (see footnote 5)

$$\frac{\text{Re } \pi_3^{(\frac{1}{2})}}{\omega^2} = -\frac{2\alpha_\epsilon m_\epsilon^2 \zeta_\epsilon^2}{\pi\omega^2} \int_1^\infty \frac{du}{2u \sqrt{u(u-1)}} \int_0^\infty \frac{d\rho}{\rho} \left\{ (2u-1) \sin^2(\rho) \cos(2u\eta) + \frac{8u(u-1)}{\lambda_\epsilon} \rho A_0 \sin(2u\eta) \right\}. \quad (63)$$

What remains is to apply the preceding method to Eq. (63). Carrying out the appropriate steps and with the help of the representation of Scorer's function [Eq. (56)] we end up with

$$\frac{\text{Re } \pi_3^{(\frac{1}{2})}}{\omega^2} \simeq -\frac{\alpha_\epsilon m_\epsilon^2 \zeta_\epsilon^{2/3}}{3\omega^2 2^{2/3}} \int_1^\infty \frac{du(8u+1)}{2u^{5/3} \sqrt{u(u-1)}} \text{Gi}'(z), \quad \frac{\text{Re } \pi_3^{(0)}}{\omega^2} \simeq -\frac{\alpha_\epsilon m_\epsilon^2 \zeta_\epsilon^{2/3}}{6\omega^2 2^{2/3}} \int_1^\infty \frac{du(4u-1)}{2u^{5/3} \sqrt{u(u-1)}} \text{Gi}'(z) \quad (64)$$

where the expression resulting from scalar QED has been included. We then consider the case $\zeta_\epsilon \gg 1$ and insert the small argument behavior of the $\text{Gi}(z)$ into Eq. (64). The obtained expression exceeds the birefringent term [Eq. (59)] by a factor $\sim (\xi_\epsilon^2/\lambda_\epsilon)^{1/3}$. According to the complementary condition [see below Eq. (55)], this factor must be much greater than unity. In correspondence, the vacuum refraction index for both helicity modes of the probe beam approaches to

$$n^{(\frac{1}{2})} \approx 1 - \frac{5\alpha_\epsilon m_\epsilon^2 \zeta_\epsilon^{2/3}}{36\sqrt{\pi}\omega^2} \left(\frac{3}{2}\right)^{2/3} \frac{\Gamma^2\left(\frac{2}{3}\right)}{\Gamma\left(\frac{13}{6}\right)} \quad n^{(0)} \approx 1 - \frac{\alpha_\epsilon m_\epsilon^2 \zeta_\epsilon^{2/3}}{36\sqrt{\pi}\omega^2} \left(\frac{3}{2}\right)^{2/3} \frac{\Gamma^2\left(\frac{2}{3}\right)}{\Gamma\left(\frac{13}{6}\right)}. \quad (65)$$

The latter result means that the vacuum in the field of a circular polarized wave, in which $\zeta_\epsilon \gg 1$, behaves like a quasi-nonbirefringent crystal where the rotation [Eq. (60)] comes from a tiny birefringent effect.

This situation is even more pronounced when the opposite condition $\zeta_\epsilon \ll 1$ is taken into account. Here the photon energy ω lies below the first pair creation threshold region where $\lambda_\epsilon \ll \xi_\epsilon^{-1} \ll 1$ but $z \gg 1$ and in correspondence one can use the large asymptotic behavior of $\text{Gi}(z)$ [given above Eq. (61)] in Eq. (64) to find that the leading order correction of the vacuum refractive index resembles the one arising in the limit of $\xi_\epsilon \lesssim 1$ [Eq. (45)]. Thus, this result ratifies our previous claim about the nonbirefringent character of the vacuum when $\zeta_\epsilon \ll 1$.

We therefore find that, in connection with the dying out of the dichroic phenomenon at $\xi_\epsilon \gg 1$, an extinction of the vacuum birefringence takes place as well. In such a case, it would be convenient to have another observable at our disposal which helps us to investigate the effects induced by the MCPs [see Secs. 5.2 and 5.3 below]. However, before we will show that the region around the first pair creation threshold, where the dichroism and birefringence are manifest, provides interesting bounds.

5. Laser-assisted search of MCPs

5.1. Perspectives in the birefringent and dichroic sector

The prospect of finding exclusion limits on the MCPs using laser technology is certainly enticing. In polarimetry, the idea is to use Eq. (19) or Eq. (41) to restrict the parametric space defined by the (ϵ, m_ϵ) plane in the way that a high-precision optical measurement of $\psi(\tau)$ or $\vartheta(\tau)$ is carried out without a significant detection of the effects induced by the MCPs. This requirement implies, for instance, that the sensitivity level in the experiment $\psi_{95\%CL}$ —which we suppose verified at 95% confidence level (CL)—is not high enough for observing the hypothetical ellipticity due to the photo-production of a $q_\epsilon^+ q_\epsilon^-$ pair. A similar idea applies when a measurement of the rotation of the polarization plane is carried out without success. As a consequence, the relations $\psi_{95\%CL} > \psi(\tau)$ and $\vartheta_{95\%CL} > \vartheta(\tau)$ [with Eqs. (19) and (41) included] must be understood as the starting point for finding out the constraints on the parameters associated with the minicharged carriers.

We start our analysis by considering the regions where the dichroism and birefringence of the vacuum are strongly manifest, i.e., where $\xi_\epsilon < 1$ and $n_* \lesssim 1$. The results coming out from this regime can be expected to be trustworthy when the bound is embedded between the dashed line, corresponding to $\epsilon m_\epsilon \xi / m_\epsilon = 1$ and the dotted line corresponding to $n_* = 1$. This region of applicability is displayed in Fig. 4 [lower white sector], which must be understood in a log-log scale. Note that the shape of this figure is generic, it does not depend on the special value of ξ chosen. Once the parameters of the strong wave are fixed, the region encompassed between the aforementioned curves cannot be studied with the approximations used in this work. Obviously, the bounds to be found in this kind of high precision

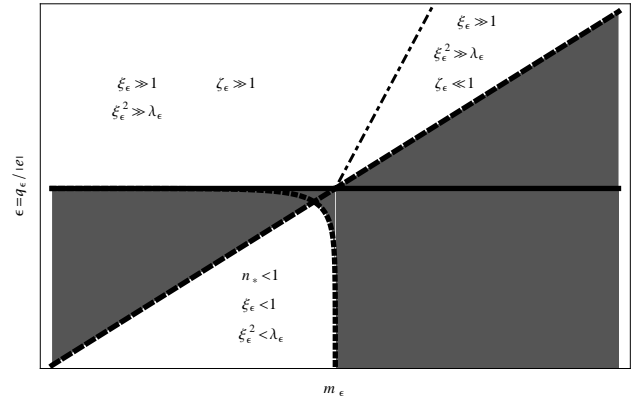


Figure 4: Regions of applicability of our calculations in the search of MCPs are indicated in the upper and lower white sectors. While the dashed line corresponds to $\epsilon m_\epsilon \xi / m_\epsilon = 1$, the solid line represents $\epsilon^2 \xi^2 = \lambda$. The dotted curve comes out from the condition associated with the first pair creation threshold $n_* = 1$. The dash-dotted line arises from the equation $\zeta_\epsilon = 1$. The gray shadow regions cannot be explored with the approximations used in this work.

optical experiment depend primarily on the intrinsic properties of both laser beams. Regarding this point we precise that, since our external field [Eq. (3)] is a monochromatic plane-wave, an appropriated experimental setup should incorporate an intense source where its oscillating period is much smaller than its temporal extension [$\tau \gg 2\pi\kappa_0^{-1}$].

So, when evaluating our expressions we have in mind an achievable experimental condition in which $\xi \approx 6.5 \times 10^{-2}$, $\tau \approx 20$ ns and $\kappa_0 \approx 1.2$ eV. Such parameters correspond to the Petawatt High-Energy Laser for heavy Ion eXperiments (PHELIX) [73], currently under operation in Darmstadt, Germany. For the probe beam we will choose an optical laser with $\omega = 2\kappa_0 \approx 2.4$ eV. In principle, this may be obtained by frequency-doubling of a portion extracted from the strong wave. Let us suppose a polarimetric experiment where the rotation [Eq. (53)] is probed. Assuming a slightly sub-resonant mass $m_\epsilon \approx 1.7$ eV [corresponding to $n_* \approx 1$], the constraint resulting for spinor MCPs is $\epsilon < 1.9 \times 10^{-6}$. On the contrary, for Klein-Gordon particles we find that $\epsilon < 2.3 \times 10^{-6}$ applies. These results have been determined by supposing the counterpropagating geometry and by considering sensitivities of the order of $\sim 10^{-10}$ rad, which appears achievable [74]. Note that for $m_\epsilon \sim 1$ eV and the relevant range of ϵ , the chosen intensity parameter ξ corresponds to $\xi_\epsilon = \xi \frac{m}{m_\epsilon} \epsilon \ll 1$. It is worth emphasizing at this point that our predictions cover regions of masses in which the constraints—deduced from several experimental collaborations—are less restrictive [11, 54]. Therefore, high-precision optical experiments in a laser wave of moderate intensities [$\xi_\epsilon \leq 1$] can complement the MCP searches at dipole magnets.

Less stringent constraints are found in the strong field regime $\xi_\epsilon \gg 1$ when the rotation of the polarization plane [Eq. (60)] is taken into account. The bounds which arise by using this expression must be consistent with the conditions $\xi_\epsilon \gg 1$, $\xi_\epsilon^2 \gg \lambda_\epsilon$ and $\lambda_\epsilon \xi_\epsilon \gg 1$ under which it was derived. Correspondingly, they have to be located far to the left of the curve $\zeta_\epsilon = \epsilon m^3 \lambda \xi / m_\epsilon^3 = 1$ but also high above the curve $\epsilon^2 \xi^2 = \lambda$. This region can be seen in Fig. 4 as well [upper white sector]. We then particularize Eq. (60) with the parameters associated with the Petawatt Optical Laser Amplifier for Radiation Intensive experimentS (POLARIS) [75], presently under operation in Jena, Germany. We remark that the intensity parameter related to this laser system is expected to reach an order of magnitude $\xi \sim 10^2$ which justifies its use in the strong field approach. This would most probably be achieved by compressing 120 J at pulse lengths $\tau_p = 120$ fs, i.e. a power near 1 PW. Moreover, this laser operates with a central wavelength $\lambda_0 = 1035$ nm corresponding to a frequency $\kappa_0 = 1.2$ eV, whose combination with its temporal length guarantees the monochromaticity condition $\kappa_0 \tau_p \gg 1$. When the probe beam is chosen as an optical laser too—similar to the Multi-Terawatt class laser JETI—[$\omega = 1.55$ eV, $\tau_J = 30$ fs] a sensitivity level $\vartheta \sim 10^{-10}$ rad seems to be reasonable [74]. By choosing $\tau = \tau_J$, we found, for Dirac Fermions $\epsilon < 6.0 \times 10^{-5}$. In contrast, for Klein-Gordon particles $\epsilon < 8.5 \times 10^{-5}$. We remark that both results apply for masses below the eV regime.

5.2. Inelastic scattered waves: the quasi-monochromatic approach

The suppression of the vacuum dichroism in the strong field regime $\xi_\epsilon \gg 1$, together with the weakness of its birefringence property, motivate us to look for an observable different from the ellipticity and the rotation of the polarization plane. Among the plausible options, we choose for counting the number of Raman-like photons which are generated from the inelastic interaction, i.e., the last two terms in Eq. (5). In this context, the rate of detected photons whose momentum differs from the incoming probe beam is given by

$$\dot{\mathcal{N}} = \dot{\mathcal{N}}_0 \mathcal{P}_{\gamma \rightarrow \gamma'} \quad (66)$$

where an optimal efficiency of detection has been assumed. Here $\dot{\mathcal{N}}_0$ denotes the number of incoming photons per unit of time and $\mathcal{P}_{\gamma \rightarrow \gamma'}$ is the respective generation probability. The latter can be computed from Eq. (5) since, on the mass-shell [$k^2 = 0$], the polarization tensor defines the photon-photon scattering amplitude with a potential change of polarization $e_1^\mu \rightarrow e_2^\mu$, i.e., $T_{e_2 k_2, e_1 k_1} = e_2^\mu \Pi_{\mu\nu}(k_2, k_1) e_1^\nu / [2V(\omega_2 \omega_1)^{1/2}]$ with the volume V where the interaction takes place. The generation of Raman-like electromagnetic waves occurs whenever $e_1 = e_2 = \Lambda_\pm / 2^{1/2}$. In correspondence, the total production rate reads

$$\mathcal{R}_{\gamma \rightarrow \gamma'} = \frac{|\pi_0(k + 2\kappa)|^2}{\omega_{\mathbf{k}+2\kappa} \omega_{\mathbf{k}}} 2\pi \delta(\omega_{\mathbf{k}} - \omega_{\mathbf{k}+2\kappa} + 2\kappa_0) + \frac{|\pi_0(k - 2\kappa)|^2}{\omega_{\mathbf{k}-2\kappa} \omega_{\mathbf{k}}} 2\pi \delta(\omega_{\mathbf{k}} - \omega_{\mathbf{k}-2\kappa} - 2\kappa_0) \quad (67)$$

where $\omega_{\mathbf{k} \pm 2\kappa} \equiv |\mathbf{k} \pm 2\kappa|$ denotes the frequencies of the Raman-like waves. Eq. (67) does not contain interference terms since the product of delta functions with different momentum contents vanishes identically. The energetic balances

imposed by the Dirac deltas in Eq. (67) cannot be fulfilled though unless \mathbf{k} and $\boldsymbol{\varkappa}$ are collinear, in which case the form factors are zero. As a consequence, the respective rate $\mathcal{R}_{\gamma \rightarrow \gamma'}$ vanishes identically always. The appearance of these Dirac's deltas is intrinsically connected with the monochromaticity of the strong field of the wave. They are distorted to another distribution functions when a finite laser pulse is taken into account. This is, in fact, the case in which we are interested in. So, in the following it must be understood that our infinite plane wave train is an approximation to the situation of practical interest, where the product of $\varkappa_0 \tau$ is very large but, on the other hand, of a finite value.

Now, the form factor involved in Eq. (67) is given by

$$\pi_0^{(\frac{1}{2})}(k \pm 2\varkappa) = -\frac{\alpha_\epsilon m_\epsilon^2 \xi_\epsilon^2}{\pi} \int_0^1 dv \int_0^\infty \frac{d\rho}{\rho} e^{-\frac{2i\rho}{|\lambda_\epsilon|(1-v^2)} [1+2A\xi_\epsilon^2] \pm 2i\rho \text{sign}[\lambda_\epsilon]} A_1 \quad (68)$$

where the quantities involved in this formula can be found in Eqs. (6)-(10). Hereafter we focus ourselves to the case where the parameter $\xi_\epsilon \gg 1$. In this context, the large asymptotic behavior of π_0 follows from the application of the method previously implemented in Secs. 3.2 and 4.3. The only difference stems in an additional factor proportional to $\text{sign}[\lambda_\epsilon]$, present in the exponent of Eq. (68). In correspondence, one finds that

$$\pi_0^{(\frac{1}{2})}(k \pm 2\varkappa) \simeq -\frac{\alpha_\epsilon m_\epsilon^2 \xi_\epsilon^{2/3}}{2^{3/3}} \int_1^\infty \frac{du}{2u^{5/3} \sqrt{u(u-1)}} \left[\text{Gi}'(z_\pm) - \frac{i}{\sqrt{3}} z_\pm K_{2/3} \left(\frac{2}{3} z_\pm^{3/2} \right) \right] \quad (69)$$

where the arguments of the special functions Gi and $K_{2/3}$ read $z_\pm = (2u/\xi_\epsilon)^{2/3} [1 \mp \lambda_\epsilon/u]$. As the expressions derived in Secs. 3.2 and 4.3, Eq. (69) applies whenever the number of absorbed photons is very large with $\xi_\epsilon^2 \gg \lambda_\epsilon$. Therefore, the bounds that emerge by using this formula must be located far to the left of the curve $\epsilon m_\epsilon \xi/m_\epsilon = 1$ but also far above from $\epsilon^2 \xi^2 = \lambda$ [see Fig. 4]. Next, for asymptotically large value of $\xi_\epsilon \gg 1$ the arguments $z_\pm \sim 0$. As long as the expansions in the small argument of Gi and $K_{2/3}$ are used, the expression above acquires the simpler structure

$$\pi_0^{(\frac{1}{2})}(k \pm 2\varkappa) \approx -\frac{\alpha_\epsilon m_\epsilon^2 \xi_\epsilon^{2/3} \Gamma^2(\frac{2}{3})}{42 \sqrt{\pi} \Gamma(\frac{7}{6})} \left(\frac{2}{3} \right)^{2/3} (1 - i\sqrt{3}). \quad (70)$$

As an outcome of the previous analysis, we observe that in the limit under consideration, $\pi_0^{(\frac{1}{2})}(k \pm 2\varkappa) \approx \pi_0^{(\frac{1}{2})}(k)$.

In order to evaluate the effects coming from the finite size of the strong laser beam, we determine the explicit solution of the equation of motion [Eq. (2)] and impose boundary conditions afterwards. A substantial simplification of the problem is achieved by ignoring the contributions given by π_1 and π_3 in Eq. (13) and keeping only the off-diagonal form factors. The diagonal quantities are then linearized according to the rules $k^2 \simeq 2\omega_{\mathbf{k}}(\omega - \omega_{\mathbf{k}})$ and $(k \pm 2\varkappa)^2 \simeq 2\omega_{\mathbf{k} \pm 2\varkappa}(\omega - \omega_{\mathbf{k} \pm 2\varkappa} \pm 2\varkappa_0)$. Observe that this last linearization applies whenever the conditions $k\varkappa \simeq 0$ and $\omega > 2\varkappa_0$ are fulfilled. In correspondence, one can deal with a simplified version of the eigenproblems given in Eqs. (12)-(14):

$$\underbrace{\begin{bmatrix} \omega_{\mathbf{k}} - \omega & -\frac{\pi_0(k)}{\omega_{\mathbf{k}}} \\ -\frac{\pi_0(k)}{\omega_{\mathbf{k}+2\varkappa}} & \omega_{\mathbf{k}+2\varkappa} - 2\varkappa_0 - \omega \end{bmatrix}}_{\mathbf{g}^{(1)}} \underbrace{\begin{bmatrix} f_+(k) \\ f_-(k+2\varkappa) \end{bmatrix}}_{\mathbf{z}^{(1)}} = 0, \quad \underbrace{\begin{bmatrix} \omega_{\mathbf{k}-2\varkappa} + 2\varkappa_0 - \omega & -\frac{\pi_0(k)}{\omega_{\mathbf{k}-2\varkappa}} \\ -\frac{\pi_0(k)}{\omega_{\mathbf{k}}} & \omega_{\mathbf{k}} - \omega \end{bmatrix}}_{\mathbf{g}^{(2)}} \underbrace{\begin{bmatrix} f_+(k-2\varkappa) \\ f_-(k) \end{bmatrix}}_{\mathbf{z}^{(2)}} = 0 \quad (71)$$

The respective eigenvalues are well approached by $\omega_1^{(1,2)} \simeq \omega_{\mathbf{k}}$ and $\omega_2^{(1,2)} \simeq \omega_{\mathbf{k} \pm 2\varkappa} \mp 2\varkappa_0$, whereas the corresponding eigenvectors are

$$\mathbf{z}_1^{(1,2)} = \frac{1}{[1 + \tan^2(\varphi_1^{(1,2)})]^{1/2}} \begin{bmatrix} 1 \\ -\tan(\varphi_1^{(1,2)}) \end{bmatrix} \quad \text{and} \quad \mathbf{z}_2^{(1,2)} = \frac{1}{[1 + \tan^2(\varphi_2^{(1,2)})]^{1/2}} \begin{bmatrix} \tan(\varphi_2^{(1,2)}) \\ 1 \end{bmatrix}. \quad (72)$$

Note that the upper indices are used to distinguish the quantities associated with each eigenproblem. We find convenient to emphasize that these eigenstates have been calculated with accuracy of terms $\sim \alpha(\alpha_\epsilon^2)$ and turn out to be parameterized by the small angles $\varphi_i^{(1,2)} \ll 1$ with $(i = 1, 2)$ and

$$\varphi_1^{(1,2)} = -\frac{f_\mp(k \pm 2\varkappa)}{f_\pm(k)} \Big|_{\omega=\omega_1^{(1,2)}} = \frac{\pi_0(k)}{\omega_{\mathbf{k} \pm 2\varkappa}(\omega_{\mathbf{k}} - \omega_{\mathbf{k} \pm 2\varkappa} \pm 2\varkappa_0)}, \quad \varphi_2^{(1,2)} = \frac{f_\pm(k)}{f_\mp(k \pm 2\varkappa)} \Big|_{\omega=\omega_2^{(1,2)}} = \frac{\pi_0(k)}{\omega_{\mathbf{k}}(\omega_{\mathbf{k}} - \omega_{\mathbf{k} \pm 2\varkappa} \pm 2\varkappa_0)}. \quad (73)$$

The previous linearizations in the dispersion equations are equivalent to reduce the differential order in the equation of motion [Eq. (2)]. In correspondence one can approach the outgoing state $\mathbf{z}^{(1,2)}$ as a superposition of the two mass eigenstates that characterize the process

$$\mathbf{z}^{(1,2)}(\omega) \simeq \sum_{\lambda=1,2} \mathcal{B}_\lambda^{(1,2)} \mathbf{z}_\lambda^{(1,2)} \delta(\omega - \omega_\lambda^{(1,2)}). \quad (74)$$

Here $\mathcal{B}_\lambda^{(1,2)}$ denote some constants to be determined by the initial conditions. For the sake of a better understanding, we Fourier transform Eq. (74) only in time. Next, we consider the experimental setup in which the incoming probe beam is a linear combination of circularly polarized waves with opposite helicities [Eq. (11)]. Besides, we suppose that at $t = 0$ only the incoming beam has a nonvanishing amplitude with $f_\pm(\mathbf{k}, 0) = [4\pi/(2\omega_\mathbf{k})]^{1/2}$. Following this procedure, one obtains a system of algebraic equations for $\mathcal{B}_\lambda^{(1,2)}$. Its solution allows to approach the components of the outgoing electromagnetic wave by

$$f_\pm(\mathbf{k}, t) = \sqrt{\frac{4\pi}{2\omega_\mathbf{k}}} \mathcal{A}_\pm(\mathbf{k}, t) e^{-i\omega_\mathbf{k}t} \quad \text{and} \quad f_\mp(\mathbf{k} \pm 2\boldsymbol{\varkappa}, t) = \sqrt{\frac{4\pi}{2\omega_{\mathbf{k} \pm 2\boldsymbol{\varkappa}}}} \mathcal{A}_\mp(\mathbf{k} \pm 2\boldsymbol{\varkappa}, t) e^{-i\omega_{\mathbf{k} \pm 2\boldsymbol{\varkappa}}t}. \quad (75)$$

The amplitudes contained in the expressions above read

$$\begin{aligned} \mathcal{A}_\pm(\mathbf{k}, t) &\approx \exp \left\{ -i\varphi_1^{(1,2)} \varphi_2^{(1,2)} \sin [(\omega_\mathbf{k} - \omega_{\mathbf{k} \pm 2\boldsymbol{\varkappa}} \pm 2\boldsymbol{\varkappa}_0) t] - 2\varphi_1^{(1,2)} \varphi_2^{(1,2)} \sin^2 \left[\frac{1}{2} (\omega_\mathbf{k} - \omega_{\mathbf{k} \pm 2\boldsymbol{\varkappa}} \pm 2\boldsymbol{\varkappa}_0) t \right] \right\}, \\ \mathcal{A}_\mp(\mathbf{k} \pm 2\boldsymbol{\varkappa}, t) &\approx -\varphi_1^{(1,2)} \sqrt{\frac{\omega_{\mathbf{k} \pm 2\boldsymbol{\varkappa}}}{\omega_\mathbf{k}}} \left\{ 2 \sin^2 \left[\frac{1}{2} (\omega_\mathbf{k} - \omega_{\mathbf{k} \pm 2\boldsymbol{\varkappa}} \pm 2\boldsymbol{\varkappa}_0) t \right] - i \sin [(\omega_\mathbf{k} - \omega_{\mathbf{k} \pm 2\boldsymbol{\varkappa}} \pm 2\boldsymbol{\varkappa}_0) t] \right\}. \end{aligned} \quad (76)$$

Clearly, the square of $\mathcal{A}_\mp(\mathbf{k} \pm 2\boldsymbol{\varkappa}, t)$ provides the photo-production probability of a Raman-like photon. The resulting expression is intrinsically associated with the exponentials responsible for the damping of the corresponding electromagnetic wave due to the mixing of photons with different helicities [second term in the exponent of $\mathcal{A}_\pm(\mathbf{k}, t)$]. We combine the respective outcomes to express the total photo-production probability of Raman-like waves as

$$\mathcal{P}_{\gamma \rightarrow \gamma'}(t) = \frac{4|\pi_0(k)|^2 \sin^2 \left[\frac{1}{2} (\omega_\mathbf{k} - \omega_{\mathbf{k} + 2\boldsymbol{\varkappa}} + 2\boldsymbol{\varkappa}_0) t \right]}{\omega_{\mathbf{k} + 2\boldsymbol{\varkappa}} \omega_\mathbf{k} (\omega_\mathbf{k} - \omega_{\mathbf{k} + 2\boldsymbol{\varkappa}} + 2\boldsymbol{\varkappa}_0)^2} + \frac{4|\pi_0(k)|^2 \sin^2 \left[\frac{1}{2} (\omega_\mathbf{k} - \omega_{\mathbf{k} - 2\boldsymbol{\varkappa}} - 2\boldsymbol{\varkappa}_0) t \right]}{\omega_{\mathbf{k} - 2\boldsymbol{\varkappa}} \omega_\mathbf{k} (\omega_\mathbf{k} - \omega_{\mathbf{k} - 2\boldsymbol{\varkappa}} - 2\boldsymbol{\varkappa}_0)^2}. \quad (77)$$

It is worth mentioning at this point that $\lim_{t \rightarrow \infty} \mathcal{P}_{\gamma \rightarrow \gamma'}(t)/t = \mathcal{R}_{\gamma \rightarrow \gamma'}$ reproduces Eq. (67). This statement can be verified by considering the relation $\pi\delta(x) = \lim_{\tau \rightarrow \infty} \sin^2(x\tau)/(x^2\tau)$.

We wish to particularize Eq. (77) to the case in which both lasers propagate quasi-parallelly, i.e., when $k\boldsymbol{\varkappa} \approx \omega\boldsymbol{\varkappa}_0\theta^2/2 \ll 1$ with θ denoting the collision angle [$\theta \ll 1$]. In this framework, the conversion probability, resulting from the substitution of Eq. (70) into Eq. (77), is given by

$$\begin{aligned} \mathcal{P}_{\gamma \rightarrow \gamma'} &= \mathcal{P}_{\omega \rightarrow \omega + 2\boldsymbol{\varkappa}_0} + \mathcal{P}_{\omega \rightarrow \omega - 2\boldsymbol{\varkappa}_0}, \\ \mathcal{P}_{\omega \rightarrow \omega \pm 2\boldsymbol{\varkappa}_0} &\approx \epsilon^{16/3} \frac{\alpha^2 \xi^{4/3} \Gamma^4 \left(\frac{2}{3} \right)}{422\pi \lambda^{2/3} \Gamma^2 \left(\frac{7}{6} \right)} \left(\frac{2}{3} \right)^{4/3} \left| 1 \pm 2 \frac{\boldsymbol{\varkappa}_0}{\omega} \right| \sin^2 \left[\frac{2m^2 \lambda}{\omega \pm 2\boldsymbol{\varkappa}_0} t \right]. \end{aligned} \quad (78)$$

We find opportune to emphasize that Eq. (78) applies for both $\omega > 2\boldsymbol{\varkappa}_0$ or $2\boldsymbol{\varkappa}_0 > \omega$. Moreover, it is valid whenever the condition $m_\epsilon \ll m [\epsilon\lambda]^{1/3}$ is fulfilled. Here the parameter λ must be understood as $\lambda \approx \omega\boldsymbol{\varkappa}_0\theta^2/(4m^2)$.

5.3. Raman spectroscopy as a probe of MCPs

Now that Eq. (77) has been established we briefly provide some details about the experimental configuration. The nature of the waves produced in the inelastic process shares certain similarities with Raman-dispersion in solid-state physics. Therefore, in the search of constraints on the MCPs it would be convenient to exploit the well known techniques of the Raman's spectroscopy. So, we suppose that after the interaction with the strong field of the high-intensity laser, the outgoing probe electromagnetic wave is picked up with a lens and sent to a monochromator. The

latter device allows us to filter out the part of the probe beam which is elastically scattered and, in correspondence, only those photons with frequency $\omega + 2\kappa_0$ or $\omega - 2\kappa_0$ are analyzed in a detector.

Let us consider the search of Raman's photons with $\omega + 2\kappa_0$. We suppose the situation in which the collision occurs with an angle $\theta \simeq 10^\circ$. Our calculations will be initially particularized with the envisaged parameters of the POLARIS system [75] [$\xi \sim 10^2$, $\kappa_0 = 1.2$ eV and $\tau_p = 120$ fs]. For the probe beam, we employ the multi-TW class laser JETI⁷, which—after a second upgrade—could deliver up to 3 J per shot in a pulse length $\tau_I \simeq 30$ fs at frequency $\omega = 1.55$ eV. Accordingly, the number of probe photons emitted per shot might reach $\mathcal{N}_0 \simeq 1.21 \times 10^{19}$. In our case, the excluded regions on the (m_ϵ, ϵ) -plane are then settled by requiring a single-Raman's photon detection for \mathcal{N} . This fact allows us to claim $\mathcal{N}/\mathcal{N}_0 > \mathcal{P}_{\gamma \rightarrow \gamma'}$. In such a case, $\mathcal{N}/\mathcal{N}_0 \approx 8.3 \times 10^{-20}$ could be established and the upper bound $\epsilon < 6.5 \times 10^{-5}$ is found for $m_\epsilon \ll 3.4$ eV. This constraint is comparable with those obtained from a polarimetric search when both lasers counterpropagate [see Sec. 5.1]. Let us consider the case in which the total measurement time is one year. Since POLARIS has a repetition rate $f_{\text{rep}} \simeq 0.1$ Hz—leading in practice to $\sigma(100)$ shots per day—one can establish the upper bound $\epsilon < 9.1 \times 10^{-6}$ for masses much below the eV-regime.

The situation could be more stringent when the envisaged experimental designations associated with the ELI and XCELS projects are considered. In these ultra-high intensity laser systems, a power $P \approx 1$ EW, with $\xi \approx 6.7 \times 10^3$ and central frequency $\kappa_0 \simeq 1.55$ eV is planned. The combination of the latter with the temporal extension $\tau \simeq 15$ fs gives us $\kappa_0\tau \approx 35$. Obviously, the monochromaticity condition is not as well satisfied as in the POLARIS case. Nonetheless, some interesting estimations can be done. For instance, by keeping the collision angle $\theta \simeq 10^\circ$ and under the assumption of a single-Raman's photon detection, it is found that an upper bound—like the best laboratory based one $\epsilon < 5 \times 10^{-7}$ [35]—would require an optical probe source delivering $\mathcal{N}_0 \sim 4 \times 10^{29}$ photons per shot. Although the latter requirement is far from the capability of the existing facilities, the fast development of laser technology offers prospects that it can be reached—even overpassed—in a near future.

6. Summary, discussion and outlook

Vacuum polarization effects induced by the interaction of MCPs and a high-intensity laser wave provide alternative scenarios for probing some low-energy effective SM extensions in which such hypothetical particles are included. In this work we have focused ourselves to the particular situation where the strong laser field is circularly polarized. We have found that in some asymptotic limits, the birefringence and dichroism of the vacuum are less pronounced than in the case in which the polarization is driven by a constant field. In particular, this holds in a region far from the threshold of pair production. Certainly, this situation is not favorable in the search of MCPs when the polarimetric techniques, with an ultra-high-intensity laser, are thought as the main experimental tools to be implemented. Nonetheless, evidences resulting from an effective Lagrangian treatment reveal a strong birefringent and dichroic character of the vacuum as the strong field of the wave is, for instance, linearly polarized. Therefore, much more severe constraints could arise. The problem, however, becomes more cumbersome because the form factors of $\Pi_{\mu\nu}$ are strongly dependent on Bessel functions [44, 51, 61]. Yet, the possibility of exploiting the quasi-static limit in the strong field regime has put forward interesting estimations [6].

In a vicinity of the region in which the photo-production of a pair occurs, the birefringent and dichroic properties of the vacuum are quite pronounced. Both phenomena are closely connected with the chiral activity of the “medium” and could be observed even at intensities available today. Observation of these elusive effects would provide evidences on the nonlinear feature of the QED vacuum. In addition, they would complement our understanding of the multi-photon pair production, already detected using nonlinear Compton scattering in the SLAC E144 experiment [78]. Moreover, at such external field strengths, the search of MCPs by using high-precision polarimetric experiments is suitable and could provide new constraints on ϵ in regions of masses where the searches based on dipole magnets are less stringent. We have shown that the latter statement applies for Dirac but also for Klein-Gordon representations of such hypothetical charge carriers. Finally, in the last part of this work, the generation of small-amplitude electromagnetic waves resulting from the inelastic part of the photon-photon scattering was investigated. We have noted that Raman's spectroscopy in a vacuum polarized by a high-intensity circular polarized laser wave could provide a sensitive probe of MCPs as well. Parameters of modern laser systems were used for establishing upper bounds on the parameters of MCPs.

⁷The feasibility of this experimental setup has been theoretically exploited in the search of Axion-like particles [76, 77].

Acknowledgments

S. Villalba-Chavez thanks Babette Döbrich for helpful discussions. He also gratefully acknowledges the support by the Alexander von Humboldt Foundation.

References

- [1] S. Weinberg. “*The Quantum theory of fields.*” **III**, Cambridge, UK: Univ. Pr., (2000), 441 p.
- [2] J. Polchinski. “*String theory.*” Vol. **I** and **II**, Cambridge, UK: Univ. Pr., (2001, 2005).
- [3] J. Jaeckel and A. Ringwald. *Ann. Rev. Nucl. Part. Sci.* **60**, 405 (2010); [arXiv:1002.0329 [hep-ph]].
- [4] J. Redondo and A. Ringwald. *Contemp. Phys.* **52**, 211 (2011); [arXiv:1011.3741 [hep-ph]].
- [5] H. Gies. *J. Phys. A* **41**, 164039 (2008); [arXiv:0711.1337 [hep-ph]].
- [6] H. Gies. *Eur. Phys. J. D* **55**, 311 (2009); [arXiv:0812.0668 [hep-ph]].
- [7] E. Witten. *Phys. Lett. B* **149**, 351 (1984).
- [8] O. Lebedev and S. Ramos Sanchez. *Phys. Lett. B* **684**, 48 (2010); [arXiv:0912.0477 [hep-ph]].
- [9] L. B. Okun. *Sov. Phys. JETP* **56**, 502 (1982); [*Zh. Eksp. Teor. Fiz.* **83** (1982) 892].
- [10] M. Ahlers, H. Gies, J. Jaeckel, J. Redondo and A. Ringwald. *Phys. Rev. D* **76**, 115005 (2007); [arXiv:0706.2836 [hep-ph]].
- [11] M. Ahlers, H. Gies, J. Jaeckel, J. Redondo, and A. Ringwald. *Phys. Rev. D* **77**, 095001 (2008); [arXiv:0711.4991 [hep-ph]].
- [12] M. Goodsell, J. Jaeckel, J. Redondo and A. Ringwald. *JHEP* **0911**, 027 (2009); [arXiv:0909.0515 [hep-ph]].
- [13] E. Dudas, Y. Mambrini, S. Pokorski and A. Romagnoni. *JHEP* **1210**, 123 (2012); [arXiv:1205.1520 [hep-ph]].
- [14] B. Holdom. *Phys. Lett. B* **166**, 196 (1986).
- [15] E. Masso and J. Redondo. *Phys. Rev. Lett.* **97**, 151802 (2006); [arXiv:hep-ph/0606163].
- [16] H. Gies, J. Jaeckel and A. Ringwald. *Phys. Rev. Lett.* **97**, 140402 (2006); [arXiv:hep-ph/0607118].
- [17] J. Jaeckel. *Phys. Rev. Lett.* **103**, 080402 (2009); [arXiv:0904.1547 [hep-ph]].
- [18] F. Brummer, J. Jaeckel and V. V. Khoze. *JHEP* **0906**, 037 (2009); [arXiv:0905.0633 [hep-ph]].
- [19] R. Cameron *et al.* *Phys. Rev. D* **47**, 3707 (1993).
- [20] E. Zavattini *et al.* [PVLAS Collaboration]. *Phys. Rev. D* **77**, 032006 (2008).
- [21] R. Battesti *et al.* *Eur. Phys. J. D* **46**, 323 (2008).
- [22] S. J. Chen *et al.* *Mod. Phys. Lett. A* **22**, 2815 (2007).
- [23] W. Dittrich and H. Gies. Springer, Heidelberg, (2000).
- [24] S. L. Adler, J. N. Bahcall, C. G. Callan and M. N. Rosenbluth. *Phys. Rev. Lett.* **25**, 1061 (1970)
- [25] A. E. Shabad. *Sov. Phys. JETP* **98**, 186 (2004).
- [26] S. Villalba-Chavez and A. E. Shabad. *Phys. Rev. D* **86**, 105040 (2012); arXiv:1206.4491 [hep-th].
- [27] S. Villalba Chávez. *Phys. Rev. D* **81**, 105019, (2010); arXiv:0910.5149 [hep-th].
- [28] K. Hattori and K. Itakura. *Ann. Phys.* **330**, 23 (2013).
- [29] A. S. Chou *et al.* [GammeV (T-969) Collaboration]. *Phys. Rev. Lett.* **100**, 080402 (2008); [arXiv:0710.3783 [hep-ex]].
- [30] J. H. Steffen and A. Upadhye. *Mod. Phys. Lett. A* **24**, 2053 (2009); [arXiv:0908.1529 [hep-ex]].
- [31] A. Afanasev *et al.* *Phys. Rev. Lett.* **101**, 120401 (2008); [arXiv:0806.2631 [hep-ex]].
- [32] P. Pugnati *et al.* [OSQAR Collaboration]. *Phys. Rev. D* **78**, 092003 (2008); [arXiv:0712.3362 [hep-ex]].
- [33] C. Robilliard *et al.* *Phys. Rev. Lett.* **99**, 190403 (2007); [arXiv:0707.1296 [hep-ex]].
- [34] M. Fouche *et al.* *Phys. Rev. D* **78**, 032013 (2008); [arXiv:0808.2800 [hep-ex]].
- [35] K. Ehret *et al.* [ALPS collaboration] *Phys. Lett. B* **689**, 149 (2010); [arXiv:1004.1313 [hep-ex]].
- [36] K. Ehret *et al.* [ALPS collaboration]. *Nucl. Instrum. Meth. A* **612**, 83 (2009); [arXiv:0905.4159 [physics.ins-det]].
- [37] K. Van Bibber, N. R. Dagdeviren, S. E. Koonin, A. Kerman and H. N. Nelson. *Phys. Rev. Lett.* **59**, 759 (1987).
- [38] S. L. Adler, J. Gamboa, F. Mendez and J. Lopez-Sarrion. *Ann. Phys.* **323**, 2851 (2008); [arXiv:0801.4739 [hep-ph]].
- [39] P. Arias, J. Jaeckel and A. Ringwald. *Phys. Rev. D* **82**, 115018 (2010); [arXiv:1009.4875 [hep-ph]].
- [40] B. Döbrich, H. Gies, N. Neitz and F. Karbstein. *Phys. Rev. Lett.* **109**, 131802 (2012); [arXiv:1203.2533 [hep-ph]].
- [41] B. Döbrich, H. Gies, N. Neitz and F. Karbstein. *Phys. Rev. D* **87**, 025022 (2013); [arXiv:1203.4986 [hep-ph]].
- [42] See: <http://www.extreme-light-infrastructure.eu>
- [43] See: <http://www.xcels.iapras.ru/>
- [44] V. N. Baĭer, A. I. Mil’shteĭn and V. M. Strakhovenko. *Zh. Eksp. Teo. Fiz.* **69**, 1893 (1975); [*Sov. Phys. JETP* **42**, 961 (1976)].
- [45] W. Becker and H. Mitter. *J. Phys. A* **8**, 1638 (1975).
- [46] G. Breit and J. A. Wheeler. *Phys. Rev.* **46**, 1087 (1934).
- [47] H. R. Reiss. *Jour. Math. Phys.* **3**, 59 (1962).
- [48] N. V. Narozhnyi, A. I. Nikishov and V. I. Ritus. [*Sov. Phys. JETP* **20**, 622 (1965)].
- [49] A. I. Titov, H. Takabe, B. Kämpfer and A. Hosaka. *Phys. Rev. Lett.* **108**, 240406 (2012).
- [50] K. Krajewska and J. Z. Kamiński. *Phys. Rev. A* **86**, 052104 (2012).
- [51] S. Villalba-Chavez and C. Müller. *Phys. Lett. B* **718**, 992, 2013; arXiv:1208.3595 [hep-ph].
- [52] A. I. Milstein, C. Müller, K. Z. Hatsagortsyan, U. D. Jentschura and C. H. Keitel. *Phys. Rev. A* **73**, 062106 (2006).
- [53] A. Di. Piazza, E. Lötstedt, A. I. Milstein and C. H. Keitel. *Phys. Rev. A* **81**, 062122 (2010).
- [54] M. Ahler, H. Gies, J. Jaeckel and A. Ringwald. *Phys. Rev. D* **75**, 035011 (2007); [hep-ph/0612098].
- [55] G. Zavattini and E. Calloni. *Eur. Phys. J. C* **62**, 459 (2009).
- [56] F. J. Dyson. *Phys. Rev.*, **75**, 1736, 1949.
- [57] J. S. Schwinger. *Proc. Nat. Acad. Sci.*, **37**, 452-455, 1951.

- [58] J. S. Schwinger. Proc. Nat. Acad. Sci., **37**, 455-459, 1951.
- [59] E. S. Fradkin in Proceeding (Trudy) of the P. N. Lebedev Physics Institute, Vol. **29**, (Consultants Bureau, New York, 1967).
- [60] R. Alkofer and L. von Smekal. Phys. Rept., **353**, 281, 2001. [arXiv:hep-ph/0007355].
- [61] V. N. Baier, V. M. Katkov and V. M. Strakhovenko. “*Electromagnetic processes at high energies in oriented single crystals.*” World Scientific, Singapore, (1998).
- [62] S. J. Orfanidis in “*Electromagnetic Waves and Antennas.*” Chap 4, online-book
<http://www.ece.rutgers.edu/~orfanidi/ewa/>
- [63] S. Ahrens, T. O. Müller, S. Villalba-Chavez, H. Bauke and C. Müller. J. Phys.: Conf. Ser. **414**, 012012, 2013.
- [64] J. L. Richard. Nuovo Cimento **8A**, 485 (1972).
- [65] T. Heinzl, B. Leifeld, K. U. Amthor, H. Schwoerer, R. Sauerbrey and A. Wipf. Opt. Comm. **267**, 318 (2006).
- [66] S. Villalba-Chavez in “*Laser-driven search of axion-like particles including vacuum polarization effects.*”; arXiv:1308.4033 [hep-ph].
- [67] A. Di Piazza, K. Z. Hatsagortsyan and C. H. Keitel, Phys. Rev. Lett. **97** (2006) 083603 [hep-ph/0602039].
- [68] I. S. Gradshteyn and I. M. Ryzhik. “*Table of Integrals, Series and Products.*” Seventh Edition, Elsevier, San Diego, (2007).
- [69] F. W. J. Olver. “*Asymptotics and special functions.*” Tenth Printing, Academic Press, London, (1974).
- [70] M. Abramowitz and I. A. Stegun. “*Handbook of Mathematical Functions.*” Tenth Printing, National Bureau of Standards, USA, (1973).
- [71] V. N. Baier, and V. M. Katkov. Nucl. Instrum. Meth. B **243**, 282 (2006).
- [72] V. I. Ritus. Ann. Phys. **69**, 55 (1972).
- [73] see: https://www.gsi.de/en/start/research/forschungsgebiete_und_experimente/appa_pni_gesundheit/plasma_physicsphelix/phelix.htm
- [74] K. Muroo *et al.* J. Opt. Soc. Am. B **20**, 2249 (2003).
- [75] M. Hornung *et al.* Appl. Phys. B **101**, 93 (2010).
- [76] B. Döbrich and H. Gies. JHEP **1010**, 022 (2010).
- [77] B. Döbrich and H. Gies. “*High-Intensity Probes of Axion-Like Particles,*” Contributed to 6th Patras Workshop on Axions, WIMPs and WISPs, Zurich, Switzerland, 5-9 Jul 2010.
- [78] D. L. Burke *et al.* Phys. Rev. Lett. **79**, 1626 (1997).